COMPILATION AND ANALYSIS OF FLIGHT CONTROL SYSTEM COMMAND INPUTS

DAVID H. WEIR

FOREWORD

This report was prepared by Systems Technology, Inc., Hawthorne, California, on Air Force Contract AF 33(615)-1818, "Compilation of Command Input Data and Investigation of Permanent Flight Control Data Exchange Program," under Task No. 821904 of Project No. 8219. The work was performed under the direction of the Flight Control Division, Air Force Flight Dynamics Laboratory, of the Research and Technology Division. The research period was May 1964 through February 1965, and the manuscript was released by the author in March 1965 as STI TR-142-1. The contractual effort was divided into two tasks — (1) Command Input Data Compilation, and (2) Permanent Flight Control Data Exchange Program Investigation. Messrs. Alonzo J. Connors and Richard O. Sickeler were the Flight Control Division project monitors for the first task reported herein.

Gratitude is extended to Messrs. R. O. Anderson and A. J. Connors of the Flight Control Division for their contributions and comments. Acknowledgment is also made to the various individuals, government agencies, and industrial groups who contributed the data presented in this report.

The project technical director was Mr. Duane McRuer, whose technical guidance was an invaluable contribution to the study. Significant contributions were also made by Mr. Claude Wezeman and Mr. Fredric Alex during the analytical interpretation phases. Finally, the author is indebted to the production staff of Systems Technology, Inc., for their careful work in preparing the manuscript.

This technical report has been reviewed and is approved.

C. B. Westbrook

C. B. WESTBROOK
Chief, Control Criteria Branch
Flight Control Division
AF Flight Dynamics Laboratory

ABSTRACT

Flight control system command input data are presented for automatic approach and landing, automatic terrain following, and manual control. The data are reduced to analytical forms useful in preliminary design where possible, e.g., power spectral densities and amplitude probability distributions. Servoanalysis methods and approximation techniques appropriate to the use of the data are discussed. Preferred data forms and areas of continuing data need are summarized.

CONTENTS

CONTENTS (Cont'd)

ILLUSTRATIONS

ILLUSTRATIONS (Cont'd)

TABLES

SYMBOLS

A_k	Amplitude coefficient
c	Pilot output
$Cy(\xi)$	Characteristic function
db	Decibels
e	System error
f	Angular frequency (cycles/sec)
f_p	Frequency of peak amplitude
$G(j\omega)$	Frequency response
$G(s)$	Transfer function
$G_f(j\omega)$	Shaping filter frequency response
$G_k(j\omega)$	Arbitrary frequency response
$G_k^*(j\omega)$	Complex conjugate of $G_k(j\omega)$
i	System forcing function or input
j	$\sqrt{-1}$
K	Transfer function gain
K_c	Controlled element gain
K_p	Pilot describing function gain
m	System output
$p(y)$	Probability density function
$P(f)$	Power
$P(\xi)$	Mellin transform of $p(y)$
$R(\tau)$	Autocorrelation function
s	Laplace transform variable, $s = \sigma + j\omega$
t	Time, independent variable
T	Time constant; time interval

T_I	Lag equalization time constant
T_L	Lead equalization time constant
T_N	Neuromuscular lag time constant
$y(t)$	Arbitrary time function; random variable
y_i	Selected value of $y(t)$
$Y(\omega)$	Fourier transform of $y(t)$
Y_c	Controlled element transfer function
Y_p	Pilot describing function
γ_c	Flight path angle command input
ζ	Damping ratio of second order system
μa	Microamperes
ξ	Dummy variable
τ	Arbitrary time lag; reaction time delay
τ_e	Effective reaction time delay
σ^2	Mean square amplitude
σ_i^2	Forcing function mean square
φ_k	Phase angle
$\Phi(f)$	Power spectral density (per cycle/sec)
$\Phi(\omega)$	Power spectral density (per rad/sec)
$\Phi_i(\omega)$	Input power spectral density
$\Phi_n(\omega)$	White noise power spectral density
$\Phi_o(\omega)$	Output power spectral density
$\Phi_{ik}(\omega)$	Cross spectral density
$\Phi_{nn_e}(\omega)$	Pilot remnant power spectral density
ω	Angular frequency (rad/sec)
$\Delta\omega$	Frequency interval
ω_i	Input bandwidth (rad/sec)
ω_k	Component frequency

SECTION I

INTRODUCTION

A. OBJECTIVE

The purpose of the report is to compile, analyze, and describe flight control system command input data for subsequent use in the preliminary design phase of advanced systems. The study is generally restricted to those critical phases of flight where the command input can be a controlling factor in specification and design. The following control modes and phases are considered:

1. Automatic control of approach and landing
2. Automatic control of terrain following
3. Manual control through fly-by-wire or stability augmenter

These are flight regimes in which the command input can require maximum maneuver capability from the airframe or high performance from the flight control system.

The data and data forms presented are directed toward flight control system preliminary design activities. Data for both the desired input and the undesired noise components are presented. Data forms having direct analytic application (e.g., power spectral density) in determining dynamic performance characteristics are evolved where possible. Failing this, forms suitable for simulation are given. The emphasis is on typical measures and bases for parameter perturbation studies.

The data presented herein have been gathered by others, and the report is fundamentally an information catalog. The data are interpreted where appropriate, and an effort is made to delimit the applicability and possible faults of the data where possible. This report is intended to complement a similar compilation, Ref. 1, of stochastic disturbance input data useful in flight control system design.

B. DEFINITION OF COMMAND INPUT

The command input gives the operating point control reference of the vehicle. The command input contains the desired reference signal, the incremental command or forcing function, systematic errors or biases, and random errors.

The functional relation of the command input is shown in Fig. 1.

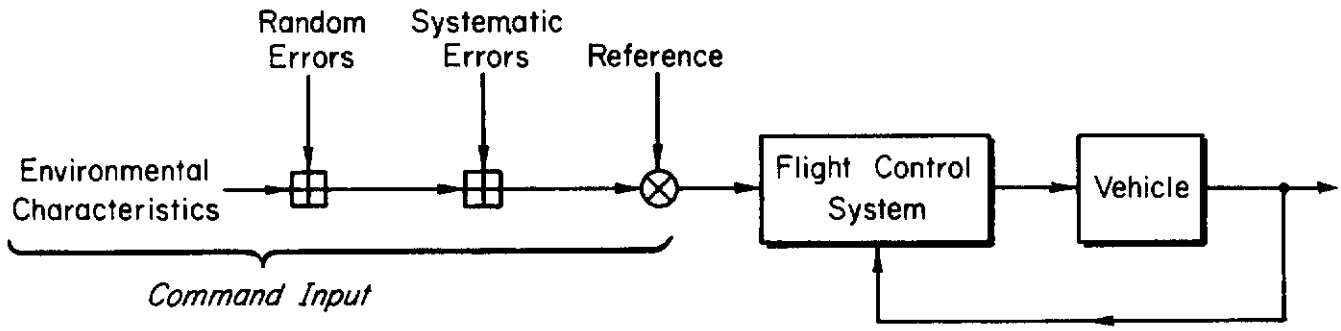

Figure 1. Command Loop Block Diagram

The controller–vehicle dynamics about the operating point are inner loop considerations, and do not lead to command inputs in this context.

C. SUMMARY OF COMMAND INPUT DATA

The data are presented in succeeding sections according to the phase of flight. Pilot inputs, present in all phases, are given separately. An index to the data contained in this report is presented in Table I.

The nature of the amplitude probability distribution is usually given when the data form is spectral density. The root mean-squared amplitude levels are given also, or they may be computed using the techniques of Section V.

TABLE I

SUMMARY OF COMMAND INPUT DATA

CONTROL MODE	FLIGHT PHASE	SYSTEM	INPUT	DATA FORM	COMPONENT	PAGE
Automatic	Approach and landing	ILS localizer	Course bending due to terrain	Spectral density	Noise	6
			Overflight interference	Deterministic waveform	Noise	7
		ILS glide path	Path bending due to terrain	Theodolite flight record	Noise	9
		Automatic landing radar	Angle noise	Spectral density	Noise	13
	Terrain following	Forward-looking radar	Terrain profile	Spectral density	Desired	16
			Scintillation	Spectral density	Noise	20
			Amplitude fluctuation	Spectral density	Noise	19
Manual	All	Fly-by-wire stability augmenter	Quasi-linear compensatory pilot model	Describing function	Desired	22
			Pilot remnant	Spectral density	Noise	25

SECTION II

APPROACH AND LANDING

A. THE INSTRUMENT LANDING SYSTEM (ILS)

The ILS system consists of three elements — a localizer radio beam to furnish directional guidance, a glide path beam for vertical guidance, and markers to provide accurate radio fixes along the approach course. Representative locations of these elements with respect to the runway are given in Fig. 2. For a more detailed description of ILS characteristics see, for example, Refs. 2 – 6.

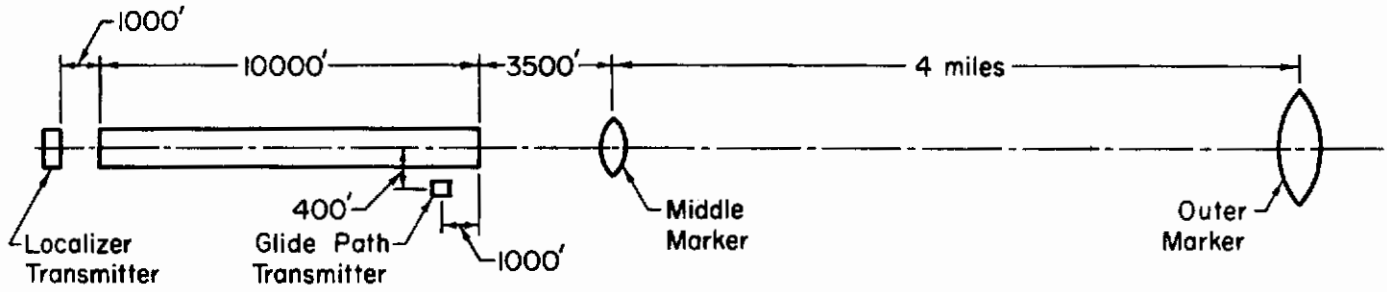

Figure 2. Typical ILS Landing Geometry

The localizer and glide path signals are received and processed on board the aircraft to provide the guidance command during approach down to established minimums. The lateral and vertical signals are either displayed on the instrument panel for manual control, or coupled directly into the flight control system for automatic control. In either case the resultant command input contains the desired signal of deviation about an ideal course down the glide path and along the runway centerline, plus undesired noise-like components due to irregularities in the beam structure. Another potential disturbance source, receiver noise, is shown in Ref. 7 to have an rms value of about 0.2 microamperes (full scale is 150 μa) and is therefore negligible.

Course and glide path irregularities are caused by beam reflections from the environment which result in a phase shift at the receiver.

The most important are due to terrain and fixed structures, since these are siting deficiencies which frequently cannot be corrected. Reflections from overflying aircraft can cause large perturbations, but appropriate traffic control procedures tend to minimize this effect. Recent efforts by the FAA have been directed toward improving the ILS course structure to permit Category III (zero-zero) landings. In connection with this, the slotted waveguide directional localizer (see Ref. 8) has come into widespread use, replacing the conventional localizer antenna.

B. ILS LOCALIZER COURSE STRUCTURE

Irregularities in the localizer course structure due to terrain reflection and other siting defects were measured by the FAA for 25 facilities in the U. S. These basic data were analyzed by Bendix in Ref. 9. The FAA data and Ref. 9 results are reanalyzed in Appendix A to place them in a format most suitable to their use as a noise component in the flight control system command input during approach.

One of the principal results of the Appendix A analysis is the power spectral density of localizer course structure variations measured at the receiver output. Individual plots for each of twelve localizer facilities are presented in Appendix A. These facilities were sufficiently self-stationary and Gaussian that the approach course could be treated as a finite sample of a stationary random process. To provide a single estimator of the spectral density characteristics, the spectral plots were averaged. The arithmetic mean was derived from the power densities in db, effectively a logarithmic transformation. The average results for nine conventional localizers are given in Fig. 3, and for three directional localizers in Fig. 4. Interfacility variability of the spectral densities is denoted in Fig. 3 by plus or minus one standard deviation limits, and in Fig. 4 by the range. Intrafacility variability is not shown.

There are several significant observations to be made from Figs. 3 and 4: (1) Both provide an indication of the noise power level. (2) The shape of Fig. 3 is approximately that of white noise in the measurement band. Some attenuation occurs at higher frequency, probably

due to course structure filtering (T = 0.5 sec) at the output of the localizer receiver (see Appendix A). Thus, the actual course structure noise is nearly flat to frequencies well beyond the bandwidth of the path modes of the airframe-autopilot closed-loop system. (3) The directional localizer noise level appears to be significantly lower at high frequency than that of the conventional localizer. Too much significance cannot be attached to a comparison of Figs. 3 and 4, however, because they are averages of different facilities. Comparison of the two antennas at the same facility in Ref. 8 showed some reduction in course noise at all frequencies with the directional system.

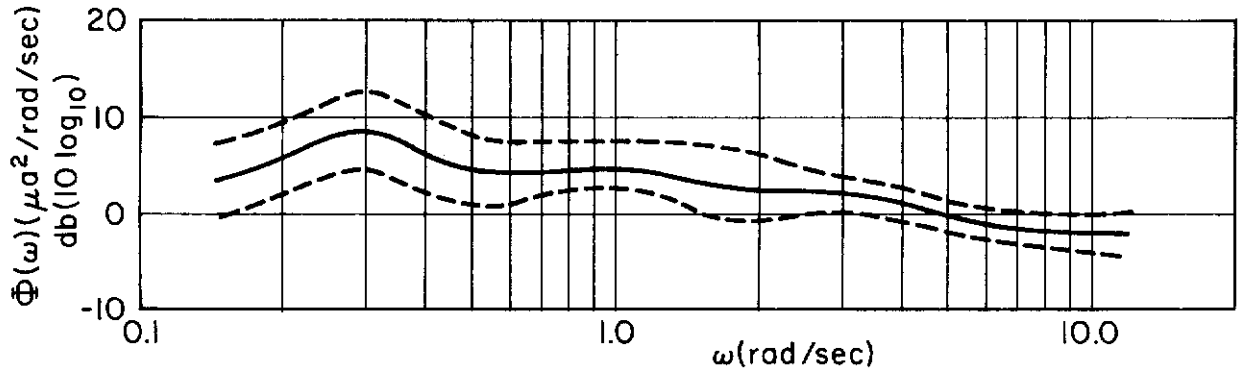

Figure 3. Average Conventional Localizer Power Spectral Density

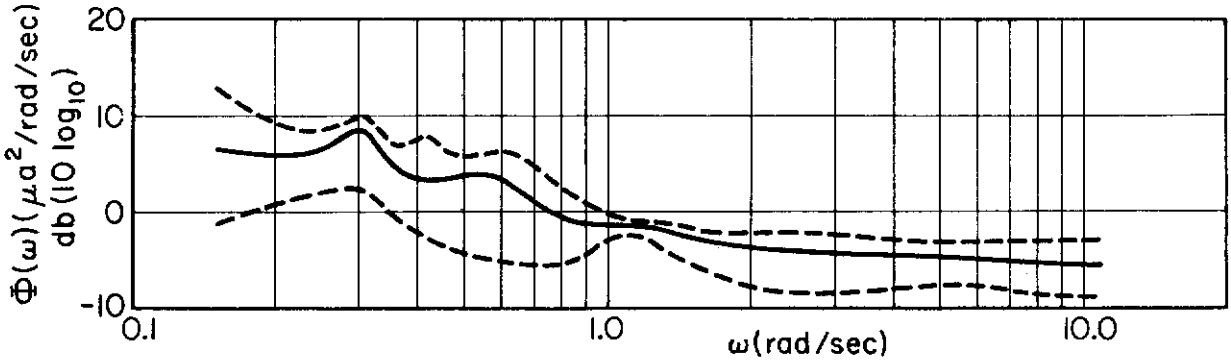

Figure 4. Average Directional Localizer Power Spectral Density

The individual spectral density plots in Appendix A were adjusted so that twice their integral gave the mean-squared value, i.e.,

$$\sigma^2 = 2\int_0^\infty \Phi(\omega)\, d\omega \qquad (1)$$

In point of fact, the integration in Eq 1 was taken only over the range for which the spectral density was known ($0.15 < \omega < 12$). Thus, integration of the average spectra in Figs. 3 and 4 will yield the average mean-square, σ^2, only if these limits of integration are used. In other words, the spectral densities of Figs. 3 and 4 are assumed to be zero for $\omega > 12$ rad/sec.

C. OVERFLIGHT INTERFERENCE IN THE ILS LOCALIZER

Reflections from aircraft flying over the runway can cause interference in the localizer receiver output of a landing aircraft. These perturbations in the course command input can become particularly significant when the overflying aircraft is at low altitude between the landing aircraft and the transmitter. The effect is most pronounced, also, when the landing aircraft is at a very low altitude just prior to touchdown. Furthermore, the variations may be greater with the more modern directional localizer, because it has a strong vertical radiation pattern along the approach path.

A detailed analysis and results pertinent to describing this interference effect as a noise-like component in the course command input are given in Appendix B. The effect is shown to be transient and not stationary, and a short term deterministic waveform is the most appropriate descriptor. General conclusions are given in Appendix B, but they are difficult to summarize because of the large number of variables. An example may serve as the best illustration.

Consider the landing aircraft at the touchdown point, with the receiver antenna height at 20 ft. Assume a DC-3 is flying across the runway halfway between the landing aircraft and the localizer antenna (track 12 of Fig. 27). The duration of the interference is approximately 5 sec from Fig. 32. The peak amplitude deviation for a 10-ft-high receiver antenna is 80 μa in Fig. 28. Adjusting this for increased antenna height by estimation from the trend of Fig. 29 yields a peak of approximately 40 μa. Assuming the waveform is that of Fig. 35(a) yields the deterministic waveform estimate shown in Fig. 5. It should be emphasized that the waveform of Fig. 5 is not unique, and that its duration and amplitude are

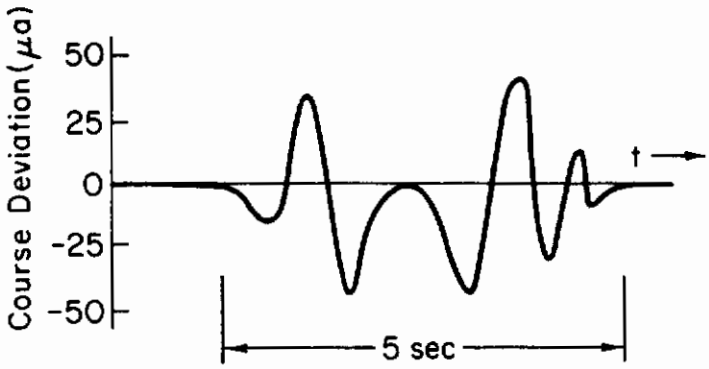

Figure 5. Example of Overflight Interference

estimates based on the assumptions of the example.

The possible consequences of overflight interference during the final stages of a Category III landing are quite severe. The probability of occurrence appears to be very small, however, for two principal reasons. First, air traffic control procedures under these conditions should be structured to keep traffic out of the interference volume (Ref. 8), and only an inadvertent penetration would make interference possible. Second, the conditions must be just right for significant disturbance to occur in the event of an inadvertent overflight. For example, the proper geometric relationship between the landing and interfering aircraft is very difficult to obtain intentionally, as discovered during the FAA experimental program (Refs. 8, 10, and 11).

Further alleviation may be obtained (as reported in Ref. 11) by utilizing longer waveguides set at higher elevations above the ground. These have the effect of replacing the single strong vertical radiation pattern of the 117-ft waveguide with several lobes of reduced intensity.

D. ILS GLIDE PATH STRUCTURE

Irregularities in the glide path structure were measured at 25 facilities in the U. S. by the FAA. The theodolite-corrected glide path deviation records formed the basic data in a study directed toward establishing dynamic performance criteria to be used in commissioning ILS facilities (Refs. 9 and 12). These records are a direct counterpart of the localizer data in Appendix A.

The inertial beam structures as functions of distance (or time at a constant velocity) are presented in Fig. 6 for eighteen of the 25 facilities. Statistical tests in Ref. 9 showed that the records from the outer marker to the runway were nonstationary. This was largely due to a significant change in both the means and variances between the middle marker and the

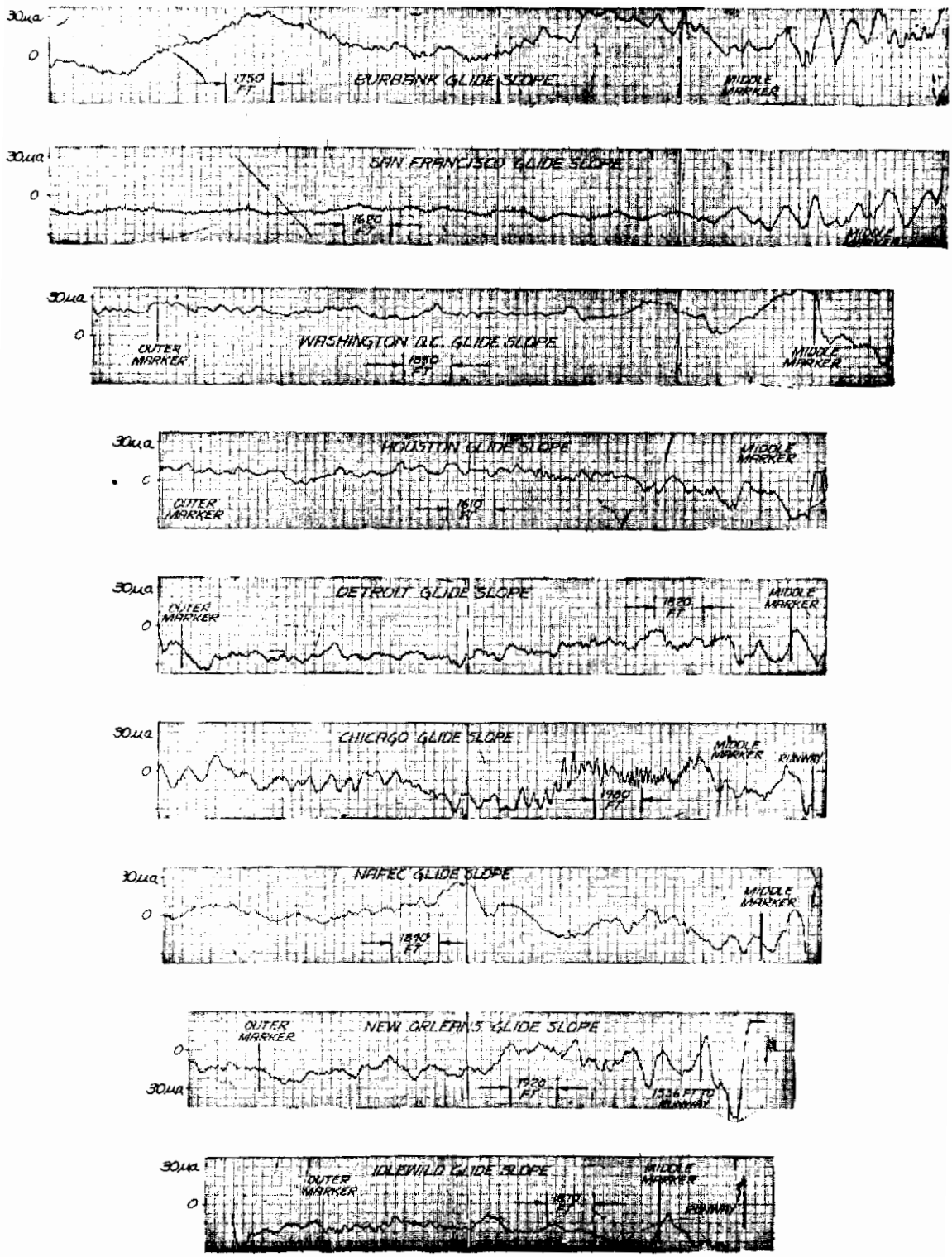

Figure 6. Theodolite-Corrected Glide Path Recordings (Ref. 9)

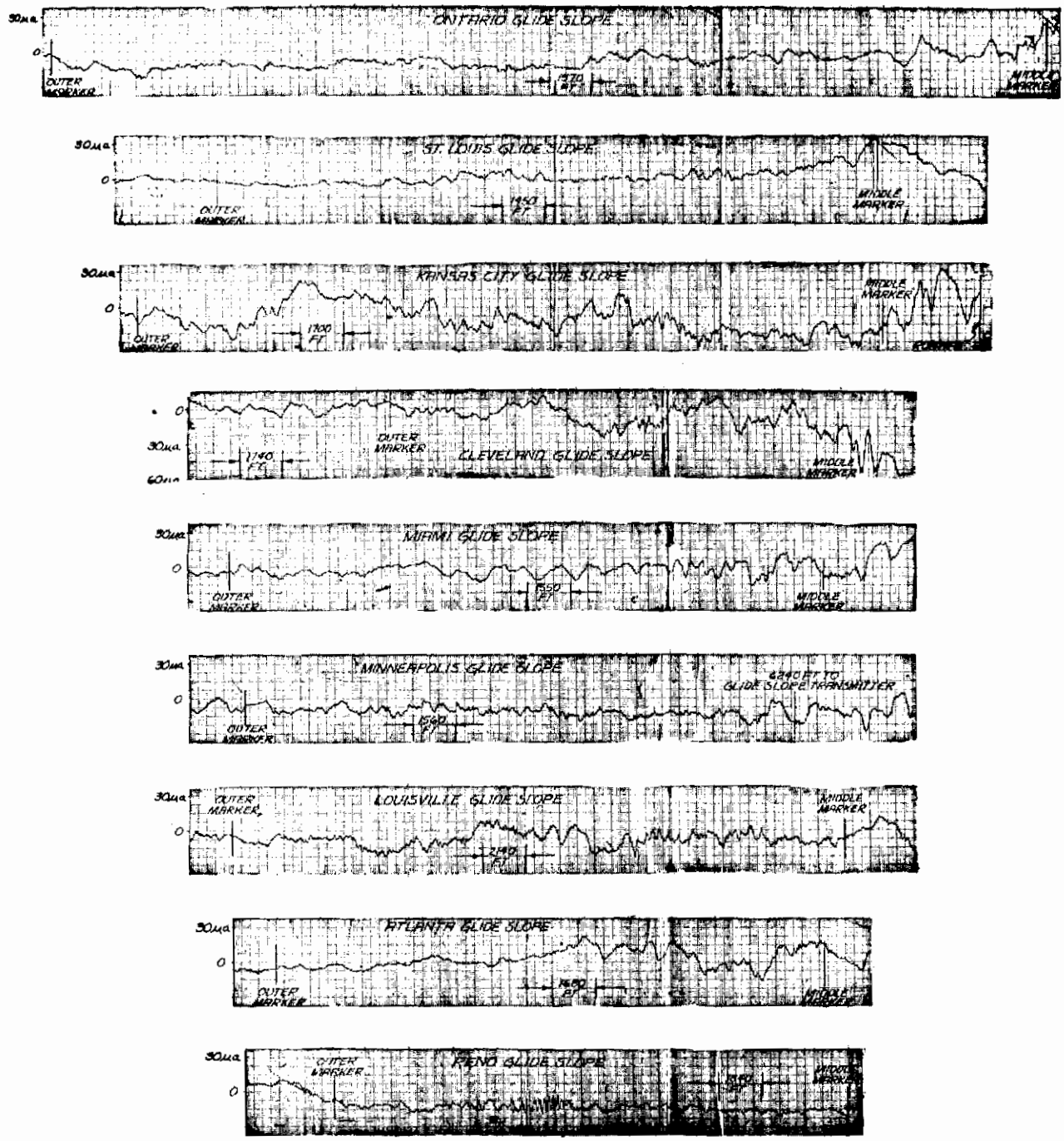

Figure 6 (continued)

runway threshold. Because the runs are nonstationary, meaningful statistical descriptors and power spectral densities are not readily derived. If only the variance changed, it might be possible to transform the data with a range-varying gain. This is analogous to desensitizing the glide path signal in the autopilot coupler (see Ref. 13). Desensitizing is not appropriate for nonstationarity in the mean, however.

To obtain statistical measures, it might be appropriate to divide the record from the outer marker to the threshold into approximately stationary subrecords. This has the disadvantage that the effective run length becomes too short, and meaningful spectral densities cannot be obtained in the low frequency region of interest.

There exists another possible basis for establishing a stationary subrecord. Current FAA planning (Ref. 14) for Category III landings indicates that the glide path will only be used down to an elevation of 70 to 100 ft. The approach and flare from that point down will be accomplished by an alternative sensor–flight-control package. This may permit truncation of the latter nonstationary portion of the glide path records for purposes of data analysis. A good discussion of the use of ILS glide path data during the final stages of the approach is presented in Ref. 13.

E. NOISE IN AUTOMATIC LANDING SYSTEMS

The primary component of the automatic landing systems for which the following data are presented is a ground-based high resolution radar. In one type of system the radar tracks the landing aircraft, determines course and glide path deviations, and transmits either these errors or corrective commands to the aircraft by radio link. This type of system can be used for approach (e.g., GCA) or fully automatic landing (e.g., Navy SPN-10 or Air Force AN/GSN-5). In another type of system (typified by REGAL, Ref. 15) the ground antenna is mechanically scanned in elevation, and a receiver in the aircraft detects (in a semiactive way) the moment that the antenna boresight is pointing at the aircraft. The aircraft elevation angle is then determined by the antenna elevation angle (transmitted via radio link) at that instant.

Angular resolution is usually the primary source of error in these systems, particularly because of the low angle above the terrain. The errors are largely a function of design characteristics, and command input noise measures which will endure in time are neither available nor appropriate. The following data are believed to be representative of equipment that entered operational use in the early 1960's.

The Bendix Radio Division conducted an analytical study (Ref. 16) of angular error sources in equipment of the REGAL type. The major part of the elevation angle error was due to:

1. Atmospheric refraction
2. Terrain reflection
3. Random antenna errors (wind, etc.)

Secondary sources of error included:

1. Receiver noise
2. Demodulation resolution and interpolation
3. Antenna angle pickoff resolution

An analytical estimate of the rms angular error in milliradians about a nominal 3 deg glide path is afforded by Table 7 of Ref. 16. The results are plotted as a function of range from the antenna in Fig. 7.

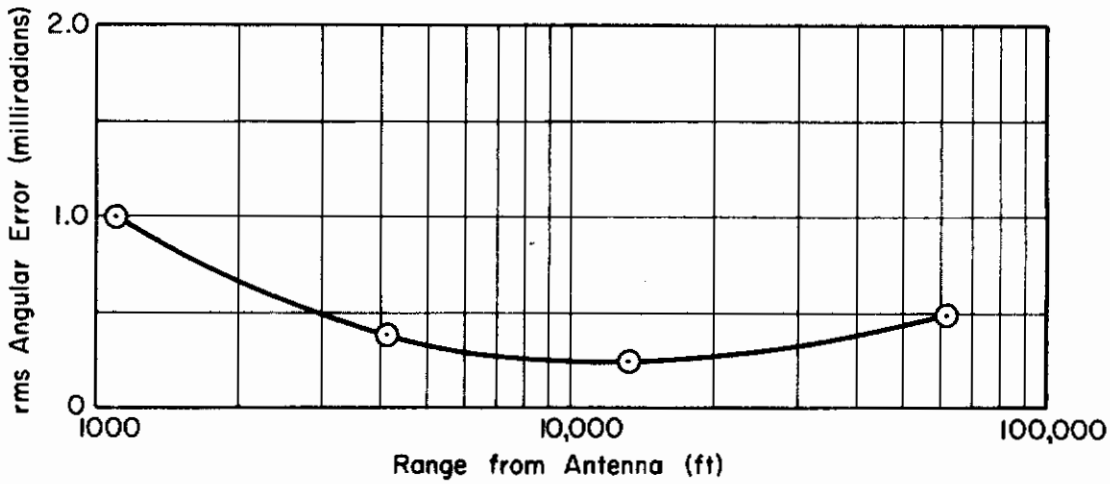

Figure 7. Idealized Angular Error (Ref. 16)

The Bell Aerosystems Company has been active for at least a decade in the development of a system for fully automatic landings. Both the Navy version, AN/SPN-10 (Ref. 17), and the Air Force version, AN/GSN-5 (Ref. 18), have a precise tracking, conical scanning radar which tracks the aircraft. Depending on the mode, either errors about the glide path or pitch and bank angle commands are transmitted to the aircraft. A corner reflector is used to eliminate scintillation, glint, and fluctuation (estimates of these errors can be obtained from Refs. 19–21).

Angular errors are the primary source of noise in the command signal of the Bell equipment. With the corner reflector or beacon tracker, the measured rms angular error is approximately 0.25 millirad (Ref. 18), and is approximately stationary with range. Other sources indicate that the frequency characteristics are well approximated by a first-order low-pass white noise shaping filter with T = 0.5 sec. The corresponding spectral density is sketched in Fig. 8.

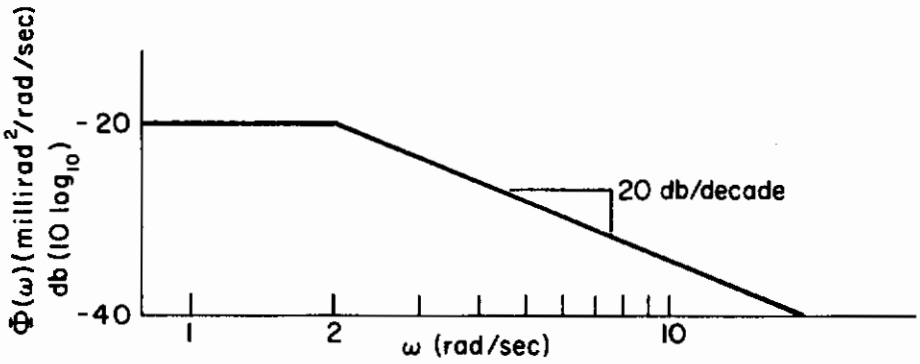

Figure 8. Typical Spectral Density for Angle Noise

SECTION III

TERRAIN FOLLOWING

A. SYSTEM CHARACTERISTICS

The terrain following command input derives from the terrain sensors and a "processor." The sensors obtain the basic terrain data ahead of the aircraft. The processor operates on the data to remove some of the noise, and to compute the command input to the flight control system. The following discussion is restricted to longitudinal maneuvers only.

The two basic types of sensors currently employed in terrain following systems are a forward-looking radar and a radio altimeter. The forward-looking radar provides the primary input for higher speed aircraft, and yields look angle to the terrain as a function of range ahead of the aircraft. The radio altimeter is normally a backup sensor in the high speed case, and provides altitude clearance at the aircraft, particularly when cresting a hill or ridge-like terrain feature. The altimeter can be used as the primary sensor in a slowly moving aircraft to provide altitude and altitude rate feedback.

The monopulse technique is most commonly used in the forward-looking radar. The principal advantages of monopulse is that its performance is largely independent of the mean signal return level of the terrain. Pencil beam radars are generally unsatisfactory, because the look angle measurement is highly dependent on the return signal strength.

B. COMMAND INPUT CHARACTERISTICS

The command input signal to the flight control system from the sensor-processor package contains signals from two sources. The first source is the external environment, resulting primarily in the terrain signal, with noise components due to scintillation and amplitude fluctuation. The second source arises in the sensor package, and its random component may be termed receiver noise. This effect is a function of the equipment design and is normally quite small.

The environment-derived signals of terrain, scintillation, and fluctuation are correlated to some extent, because they are related to and vary with the characteristics of the terrain. Similarly, they are correlated with the disturbance inputs due to gusts, because the nature of the atmospheric turbulence is related to the type of terrain (mountainous, farmlands, etc.). Thus, one is not free to choose the various inputs independently, but should select the form and study perturbations with due regard to their interaction.

1. Terrain Profile Data

The basic form of terrain data consists of the geographic terrain profile given as height versus range or distance along the profile. This type of data is readily obtainable from a topographic map. A course near the Naval Ordnance Test Station, China Lake, California, is widely used for both simulation studies and experimental testing because of its exceptional roughness. Called NOTS Course 10, it extends over a range of about 50 nautical miles in a straight line from before Bear Mountain to beyond Cross Mountain.

The actual profile for NOTS Course 10 is tabulated in Appendix C through the courtesy of NOTS personnel (Ref. 22). The tabulation starts at a range of 54,173 ft, because the preceding part of the course is essentially flat.

The power spectral density was computed by NOTS for both the complete Course 10 and for a truncated version without Bear Mountain in the profile (to make it somewhat more homogeneous). These data are presented in Fig. 9. The complete Course 10 spectrum includes all the data of Appendix C, while the spectrum for the shorter course truncates all profile points before range 104,000 ft. Asymptotes for second-order shaping filter approximations are also given in Fig. 9, as are the mean squares.

2. Flight Path Angle Command Data

A detailed analysis of terrain data viewed in the context of the resultant flight path angle command is presented in Appendix D, based on studies by the Cornell Aeronautical Laboratory. It is shown that an

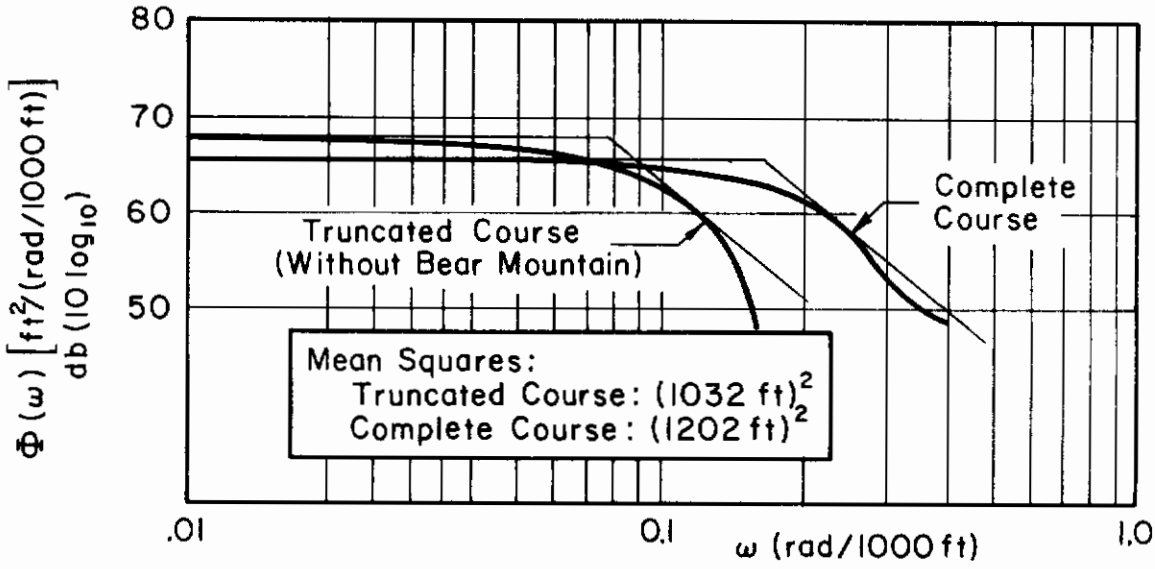

Figure 9. NOTS Course 10 Power Spectral Densities

"ideal profile trajectory" above the actual terrain can be used to obtain a flight path angle command input, γ_c, which is optimum in some sense. Power spectral densities of this command input are presented for representative terrain at several different aircraft speeds and assumed acceleration limits. These spectra are insensitive to the dynamics of the aircraft over a broad range, since they define the desired or reference trajectory based on kinematic considerations.

Spectral densities of the ideal profile γ_c are derived in Appendix D for Southern Pennsylvania (6201) and Rocky Mountain (9998) terrain. Both are moderately rough and are indicative of a demanding terrain following task. The effect of aircraft speed on the shape of the γ_c spectrum for one terrain is small (see Figs. 39 and 40). The difference in spectral characteristics between the 6201 and 9998 data is much larger. Spectra for γ_c at a velocity of 0.9 Mach and with acceleration limits of +1g and −0.5g are presented in Fig. 10 for the two terrains (abstracted from Appendix D). The 9998 profile is seen to have substantially more power at low frequency. The high frequency characteristics are nearly coincident. The second-order white noise shaping filters shown are adapted from Appendix D.

Although Fig. 9 represents height and Fig. 10 is proportional to the derivative of terrain height, they both have the shape of second-order

shaping filters. This is because Fig. 10 includes the effective equalization dynamics of the processor, not just the derivative of the terrain height.

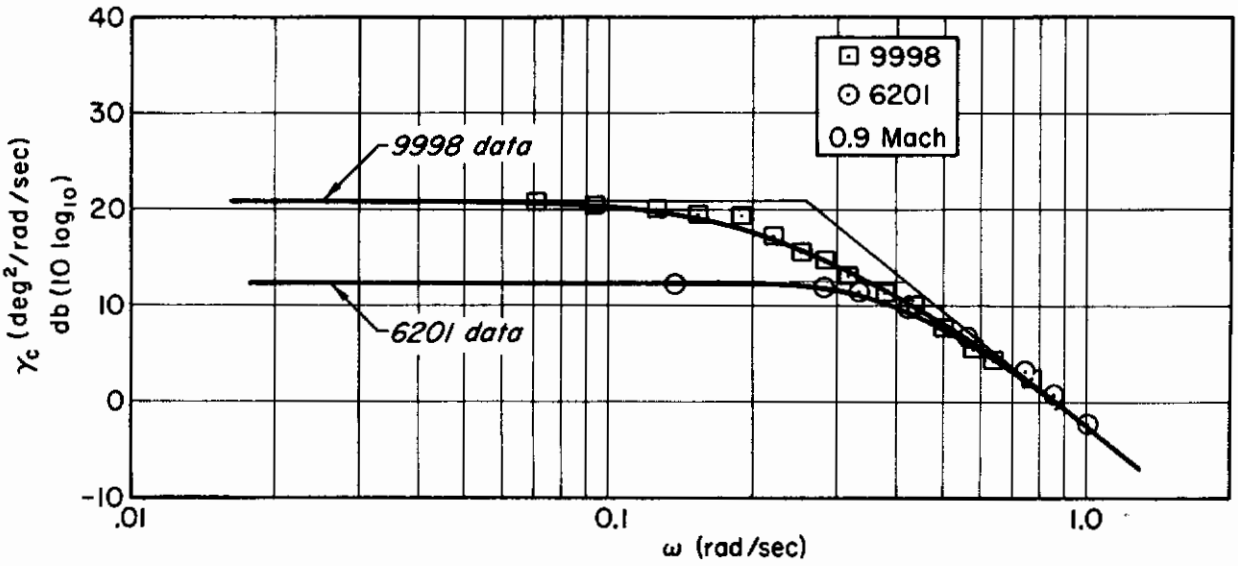

Figure 10. Power Spectral Densities of γ_c for Ideal Profiles (Appen. D)

It is generally agreed that the terrain "process" is both stationary and Gaussian over a distance of a few miles about the mean terrain slope. The terrain tends to be "cuspy," however, with sharp peaks and rounded valleys. Derivation of the ideal profile is effectively a filtering process, and it tends to eliminate the cuspiness, making the terrain more Gaussian. This characteristic is convenient in linear systems analysis, allowing computation of rms performance indices.

Other probability distributions encountered in terrain data (e.g., Rayleigh and rectangular) are more difficult analytically, but can be simulated. Some terrain features are not well described as a random process (e.g., towers, cliffs, smokestacks), and are better represented by equivalent deterministic inputs for either analytical or simulation studies.

3. Amplitude Fluctuation

Amplitude fluctuation is a variation in the amplitude or power of the radar return signal from the terrain, and it can have an indirect effect on the command input. The variation in amplitude fluctuation with terrain characteristics is illustrated for S-band radar in Fig. 11 (adapted from Ref. 23). The probability density is plotted as a function of normalized return power (i.e., power divided by average power).

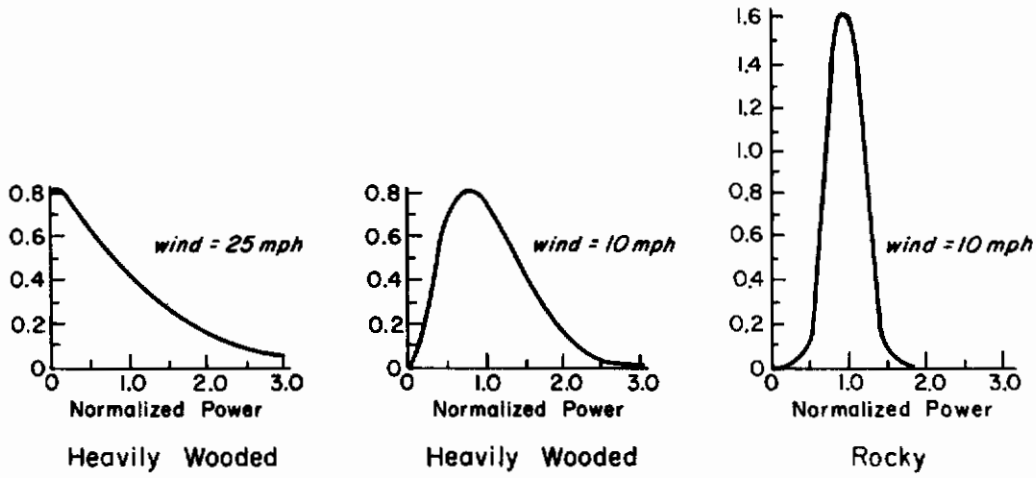

Figure 11. Probability Density of Amplitude Fluctuation (Ref. 23)

The increase in random fluctuation due to wind and foliage is readily seen. For leafy terrain in a strong breeze the individual scatterers are free to change phase and orientation, and the return is nearly random. In a light breeze (10 mph) there is some randomness with bunching about the average power. For rocky terrain there is little randomness, and only a slight fluctuation in power. Monopulse radar techniques tend to minimize the effect of amplitude fluctuation. Over smooth terrain (calm water or a sandy desert) there may be a large amount of specular reflection and little back-scattered energy. In this case the signal level may be undetectable or at best unreliable, and forward-looking radar techniques are ineffective.

The influence of wind speed on the fluctuation power spectrum is illustrated in Fig. 12 (taken from Ref. 23). The spectral amplitude for

each wind speed is normalized with respect to the steady or average power at that speed. As the wind increases, the random power increases relative to the average power level. This increase in fluctuation results in a decrease in the angular resolution (particularly for nonmonopulse systems) which can lead in turn to uncertainty or errors in the FCS command input. One function of the sensor-processor package is to reduce this type of error.

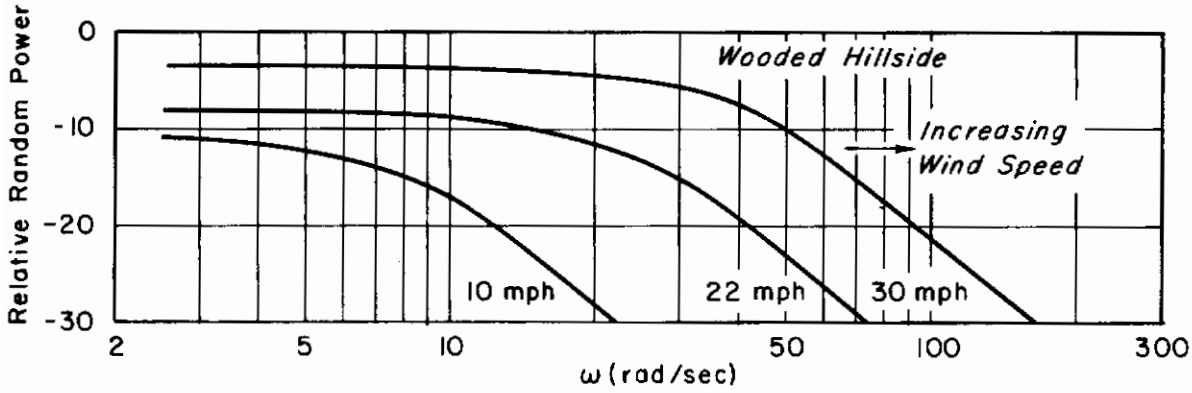

Figure 12. Amplitude Fluctuation Spectral Density (Ref. 23)

The data of Figs. 11 and 12 are only intended to illustrate the effect of environment on the random component of the signal. The average signal level would be needed, as well, for direct application of these data to a specific design problem.

4. Scintillation

Scintillation is a variation in the apparent look angle of the radar sensor due to angular scattering of the return signal from the terrain. This phenomenon is particularly significant with heavily vegetated terrain where the leaves behave as individual scatterers. It is important over rocky slopes, ocean waves, etc., where there are small scattering surfaces oriented in random ways. Scintillation is characteristically a random process, and is well suited to statistical and spectral description.

A typical example of the angular amplitude probability distribution is given in Fig. 13 for vegetated terrain. An example of scintillation spectral density for vegetated terrain is given in Fig. 14. The bandwidth

is a function of wind speed for leafy terrain and water waves (for example), as is the total scintillation power or rms angular variation.

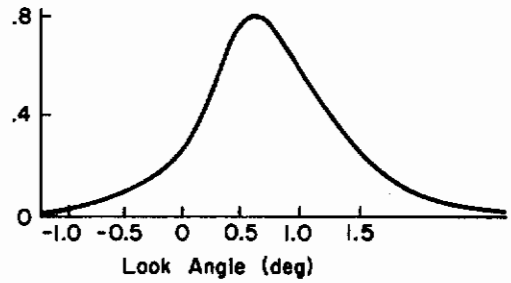

Figure 13. Probability Density of Scintillation

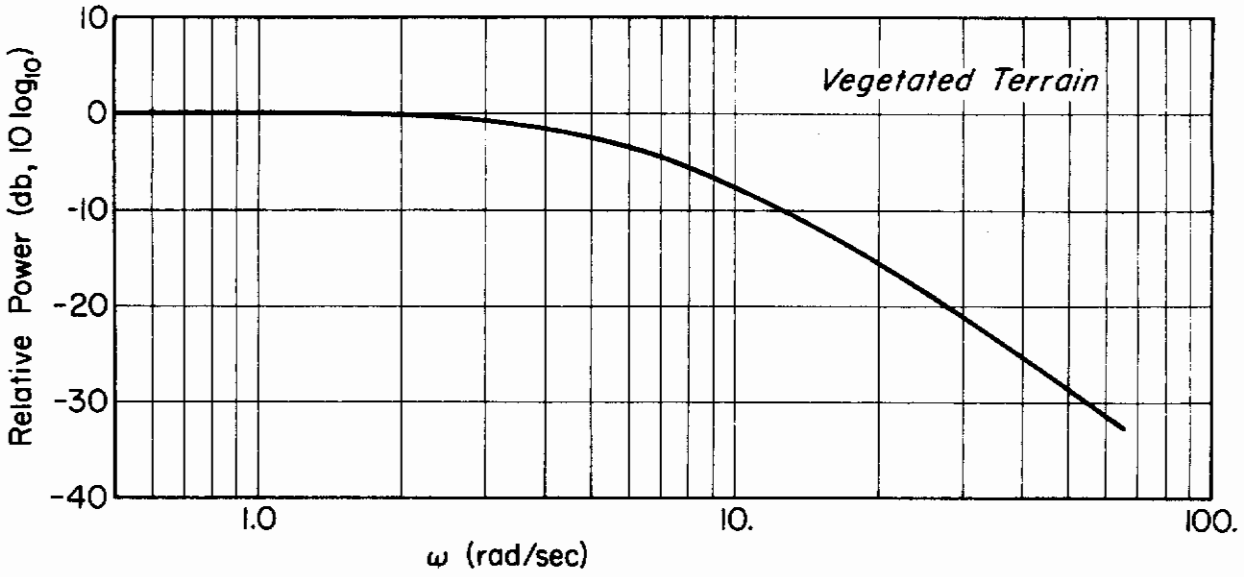

Figure 14. Scintillation Spectral Density

Low frequency scintillation is likely to be present as a noise component in γ_c from the sensor–processor package. It is difficult to distinguish from terrain variations and, unlike amplitude fluctuation, it is not minimized by monopulse radar techniques. These data are only illustrative, and the exact amount of angular error in the command input in a given application is a function of the design of the processor. A more complete analysis and details on specific systems are presented in Ref. 24.

SECTION IV

MANUAL CONTROL

A. THE PILOT AS A SOURCE OF COMMAND INPUTS

Pilot-derived inputs (both desired and undesired) are an important factor in the design of flight control systems for advanced vehicles, including fly-by-wire and stability augmentation. It is essential to present the pilot with good system response characteristics. This constrains system bandwidth, nonlinearities, authority, surface deflection rates, etc. The undesired pilot input (or remnant) can be a large source of excitation for flexible and higher frequency rigid-body modes of the vehicle.

The pilot is well characterized by a quasi-linear describing function-plus-remnant model. This model is given in block diagram form for a compensatory single-loop tracking task in Fig. 15. The form of the model may vary with the nature of the display (e.g., pursuit versus compensatory) and the multiplicity of the task. The model parameters vary (at least) with controlled element (controller–vehicle) dynamics, manipulator dynamics, and forcing function (input) amplitude and frequency. The describing function is the critical factor in determining pilot–system stability. The remnant can be important to measures of system performance such as the mean-squared error.

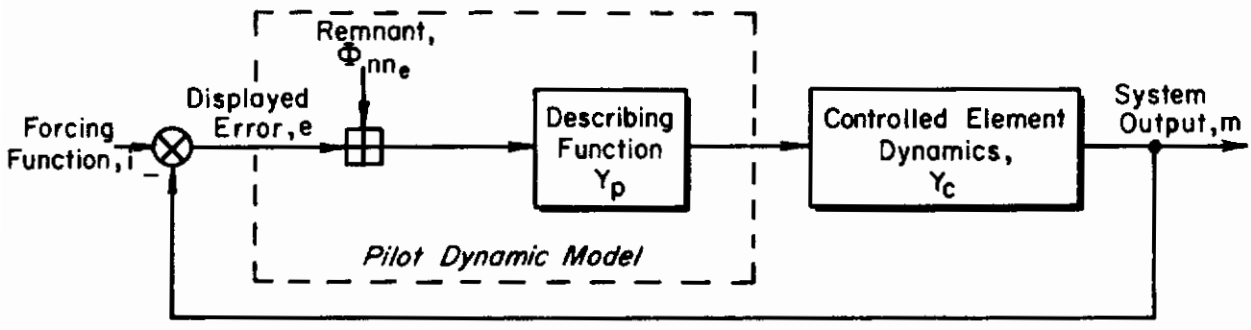

Figure 15. Pilot Control in Compensatory Task

B. PILOT DESCRIBING FUNCTION

The describing function characterizes that part of the pilot's transfer characteristics which is linearly correlated with the forcing function. There are two elements to this part of the model, a generalized describing function form and a set of adjustment rules.

A very complete generalized describing function is presented and discussed thoroughly in Ref. 25. A somewhat simplified version that still has general applicability is adequate for this discussion. A good approximation (taken from Ref. 25) to the describing function form is given by

$$Y_p = \frac{K_p(T_L j\omega + 1)e^{-j\omega\tau}}{(T_I j\omega + 1)(T_N j\omega + 1)} \qquad (2)$$

where K_p = gain

τ = reaction time delay

$\frac{(T_L j\omega + 1)}{(T_I j\omega + 1)}$ = equalization characteristic

$\frac{1}{(T_N j\omega + 1)}$ = neuromuscular system characteristic

This version, Eq 2, neglects the indifference threshold, higher order neuromuscular effects, and a very low frequency lag characteristic.

Complete adjustment rules are given in Ref. 25, but they can be briefly summarized. The pilot describing function adopted for a given task is very similar to that which a servo engineer would select given the controlled element and a controller "black box" having the form of Eq 2 and knobs for T_I, T_L, and K_p. Under appropriate conditions this reduces to the "crossover model," in which Y_p is selected so that the linear forward loop transmission, Y_pY_c, is approximately $Ke^{-j\omega\tau}/j\omega$ in the region of crossover.

C. PILOT REMNANT

1. Importance

The remnant is that portion of the pilot's output which is not linearly correlated with the forcing function. It is always present, and it is probably the most significant undesired input into the primary and fly-by-wire flight control systems from a practical standpoint.

The remnant can have significant power at frequencies that are high enough to excite low frequency flexible modes of the airframe. Recent controlled element transition data (Ref. 26) show that the pilot can identify a new Y_c and readapt his describing function within a very few seconds. This suggests that he may be dither adaptive, identifying the system dynamics with his high frequency remnant power.

2. Sources

The major source of remnant appears to be nonstationarity in the pilot's behavior (Ref. 25). This is manifest as time-varying components in the gain, K_p, and the effective time delay, τ_e. A time-varying gain results in variation in the amplitude ratio of the pilot describing function data at low frequency. Time variation in τ results in low frequency variation of the describing function phase angle data.

Some evidence exists for pulsing behavior by the pilot in the output amplitude distribution for control of second-order systems, e.g., $Y_c = K/(j\omega)^2$. This indicates a tendency for the pilot's output to be pulses with areas roughly proportional to the stimulus amplitude. This is an additional remnant source for this type of Y_c.

A number of the experiments in Ref. 25 were designed to show sampling or nonlinear behavior of the pilot. Careful examination of the output spectral density out to a frequency of 46 rad/sec, however, showed no evidence of sampling. Nonlinear behavior would be evidenced by the appearance in the output of higher harmonics for the input sinusoids, almost by definition. No harmonic peaks were present in the data. Thus, the hypotheses of remnant explanation by sampling or nonlinear behavior were rejected.

3. Data

The remnant is considered to be a power spectrum injected at the operator's input for modeling purposes, denoted by Φ_{nn_e} in Fig. 15. The point of application could be moved to other places in the loop as long as no nonlinear elements are passed in the process; however, the remnant spectra for a wide variety of controlled elements coalesce best when reflected to the pilot's input (Ref. 25).

Compilation of an extensive body of remnant data reflected to the pilot's input is given in Fig. 16. The data points (circles, diamonds, etc.) were obtained from the experimental program reported in Ref. 25. The data depicted by lines derived from a completely independent study accomplished by Elkind, Ref. 27. The plot gives the power spectral density normalized with respect to the forcing function mean square.

The Ref. 25 data points correspond to various controlled elements. The forcing function was a random-appearing spectrum with a cutoff frequency, ω_i, of 2.5 rad/sec, generated by a sum of sinusoids. The Ref. 27 lines were for a simple gain controlled element and random-appearing input spectra composed of sums of sinusoids with three different cutoff frequencies.

Several trends are apparent from Fig. 16. The remnant power increases with controlled element gain and order, and decreases with forcing function bandwidth. For extreme controlled element forms such as

$$Y_c = \frac{K_c}{j\omega(j\omega - 1.5)}$$

the remnant increases greatly. This may be interpreted as a result of the increasingly time-varying behavior adopted by the pilot in an attempt to retain control.

Values of the remnant computed at the forcing function frequencies (sinusoidal components) generally fit a smooth curve through values measured between and above forcing function frequencies. This indicates that the power spectral density of the remnant is continuous and that significant line spectra are absent.

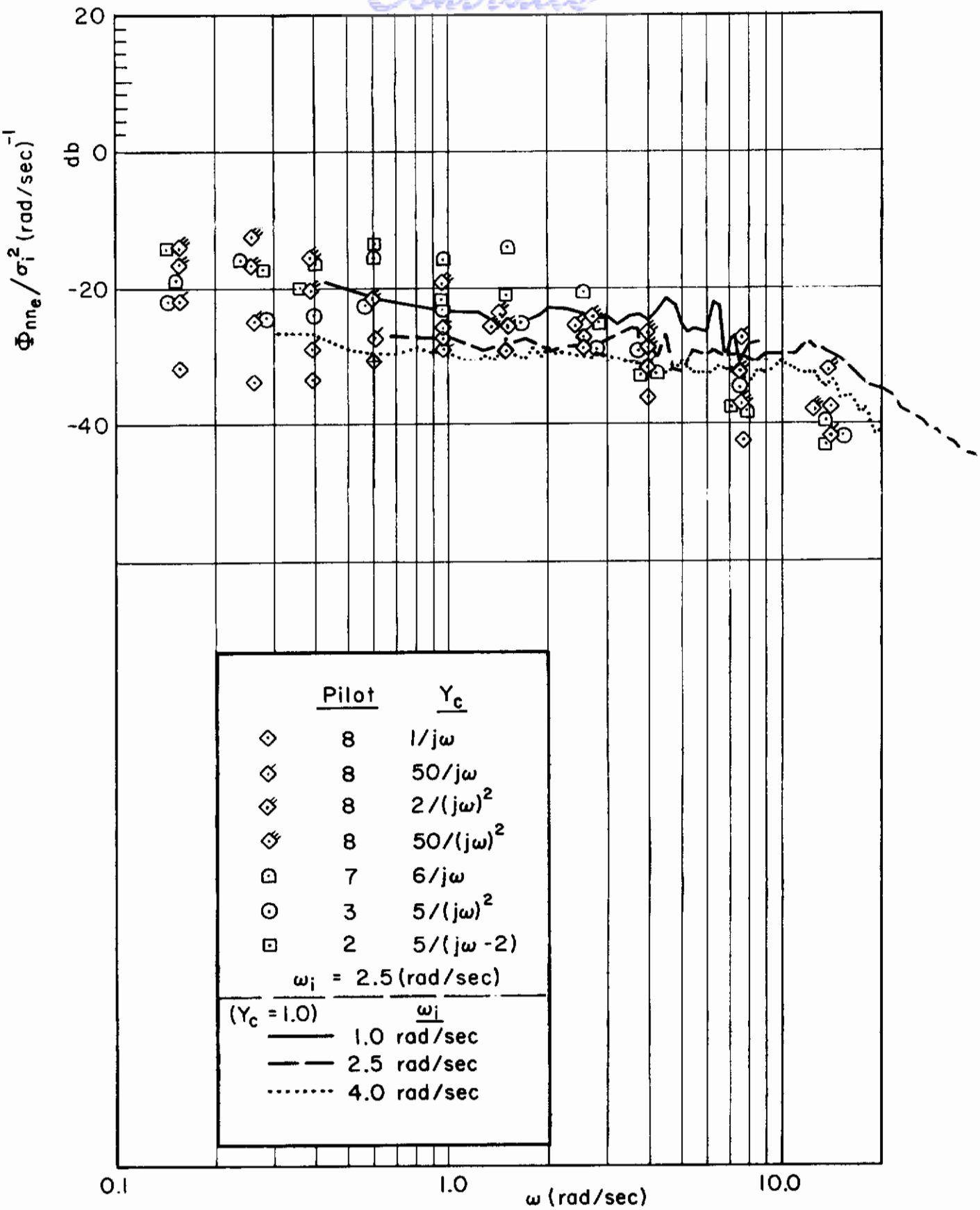

Figure 16. Pilot Remnant Data (Refs. 25 and 27)

SECTION V

APPLICATION TO FCS ANALYSIS

A. DATA FORMS

There are several command input data forms appropriate to the analysis of flight control systems. These include:

1. Deterministic descriptors
2. Amplitude probability distributions
3. Autocorrelation functions
4. Power spectral densities

Examples of all but the autocorrelation function are found in the data of preceding sections.

Succeeding subsections summarize the ways in which each form of data may be used in flight control analysis. This frequently is accomplished by direct application of the extant data form. It may involve reduction of the data from one form to a more useful equivalent. Approximation by a simpler form is often highly advantageous. The relation between the several forms is indicated to a degree compatible with the brevity of this exposition.

The following summary provides the definitions and relations appropriate to interpretation of the data. The indicated references should be adequate to provide background and supporting detail.

B. CONVENTIONAL ANALYSIS TECHNIQUES

Thorough treatment of standard servoanalysis techniques may be found in Ref. 28 for linear systems, and in Ref. 29 for nonlinear systems. An excellent series of reports useful in preliminary design of flight control systems is given by Refs. 30 – 32. These reports fully define the methods of analysis. A summary of dynamic performance criteria for random and deterministic inputs is given by Refs. 33 and 34, respectively.

1. Frequency Characteristics of Random Inputs

The command input is often well approximated as a finite sample in time of a stationary random process. If the run length is sufficiently long and the process is both Gaussian and ergodic, a powerful body of analytic techniques may be called forth (e.g., Refs. 35–38).

The most useful descriptor of random data is the power spectrum. It can be obtained from a single time function, $y(t)$, of an ergodic process using the time average autocorrelation function, i.e.,

$$R(\tau) = \lim_{T\to\infty} \frac{1}{T} \int_{-T/2}^{T/2} y(t)y(t+\tau)\, dt \qquad (3)$$

where T is the averaging interval. If $y(t)$ can be written in the Fourier integral form

$$y(t) = \int_{-\infty}^{\infty} Y(\omega)e^{j\omega\tau} \frac{d\omega}{2\pi} \qquad (4)$$

where

$$Y(\omega) = \int_{-\infty}^{\infty} y(t)e^{-j\omega t}\, dt$$

then substituting Eq 4 into Eq 3 and taking the limit for large T, $R(\tau)$ becomes the Fourier transform of the power spectral density (after Ref. 38), i.e.,

$$R(\tau) = \int_{-\infty}^{\infty} \Phi(\omega)e^{j\omega\tau}\, d\tau$$

Taking the inverse Fourier transform yields by definition:

$$\Phi(\omega) = \frac{1}{2\pi} \int_{-\infty}^{\infty} R(\tau)e^{-j\omega\tau}\, d\tau$$

Restricting $y(t)$ to be real and recognizing that $R(\tau)$ and $\Phi(\omega)$ are even

functions yields the Fourier transform pair

$$R(\tau) = 2\int_0^\infty \Phi(\omega) \cos \omega\tau \, d\omega$$

$$\Phi(\omega) = \frac{1}{\pi}\int_0^\infty R(\tau) \cos \omega\tau \, d\tau \qquad (5)$$

The mean-squared amplitude, σ^2, for a stationary y(t) is R(0) or the integral of the power spectral density, i.e.,

$$\sigma^2 = R(0) = 2\int_0^\infty \Phi(\omega) \, d\omega \qquad (6)$$

This expression holds for all data presented in this report.

The spectral density of the output, $\Phi_o(\omega)$, of a linear transfer element can be obtained in terms of the input. Consider the simple block diagram of Fig. 17, where G(s) might represent a controller–vehicle closed-loop transfer characteristic in the presence of a command input spectrum, $\Phi_i(\omega)$. The output spectrum, $\Phi_o(\omega)$, is given by the relation

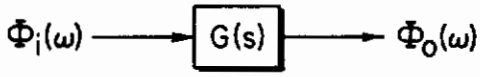

Figure 17. Simple Transfer Characteristic

$$\Phi_o(\omega) = |G(j\omega)|^2 \, \Phi_i(\omega) \qquad (7)$$

An immediate application of Eq 7 is the computation of mean-squared amplitude for an output quantity in the presence of the command input, $\Phi_i(\omega)$. This is accomplished by evaluating Eq 6 for $\Phi_o(\omega)$ to obtain σ^2, or the rms, σ. This technique allows computation of a variety of performance indices. Examples include flight path deviation about the ideal profile in terrain following, or the localizer course in an automatic approach. Design considerations such as rms surface deflection and deflection rate can be studied as well.

Another application of Eq 7 is in the modeling of the command input spectral density. If $\Phi_n(\omega)$ is a Gaussian white noise source, then a

shaping filter, $G_f(j\omega)$, can be "fitted" to yield the command input spectrum, $\Phi_i(\omega)$, to a selected degree of approximation. The input spectrum is given by

$$\Phi_i(\omega) = |G_f(j\omega)|^2 \Phi_n(\omega) \tag{8}$$

Since $\Phi_n(\omega)$ is a constant, $|G_f(j\omega)|^2$ has the shape of the input spectrum.

A more general case is the one where the command input is the sum of several random signals. For N input components and one output, the transfer function characteristic of Fig. 17 becomes that shown in Fig. 18. The inputs are assumed to have zero means, but are not necessarily uncorrelated. Denote the cross-spectral density between the ith and kth inputs as $\Phi_{ik}(\omega)$. Defining $G_k^*(j\omega)$ as the complex conjugate of $G_k(j\omega)$, yields the following equation for the output spectrum:

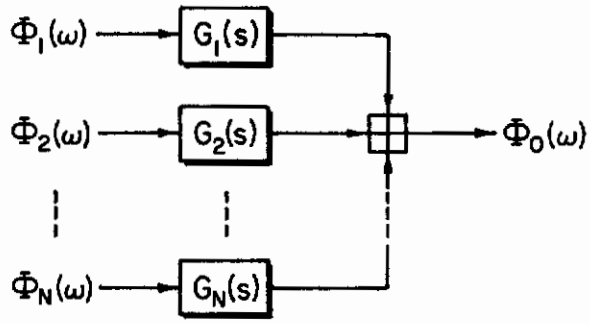

Figure 18. Multiple-Input System

$$\Phi_o(\omega) = \sum_{i=1}^{N} \sum_{k=1}^{N} G_i(j\omega) G_k^*(j\omega) \Phi_{ik}(\omega) \tag{9}$$

When the N inputs are uncorrelated, Eq 9 reduces to:

$$\Phi_o(\omega) = \sum_{k=1}^{N} |G_k(j\omega)|^2 \Phi_k(\omega) \tag{10}$$

If the inputs are summed prior to entering a single transfer block, Fig. 18 becomes that given in Fig. 19:

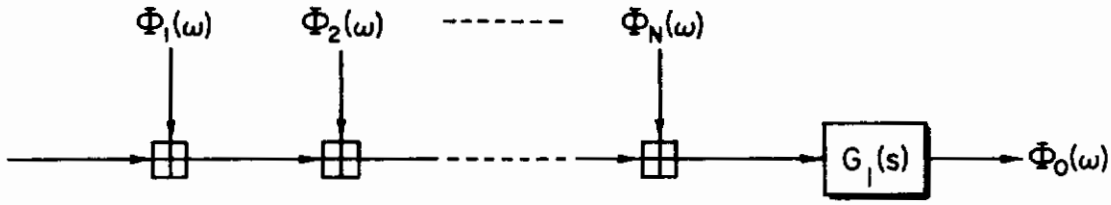

Figure 19. Summation of Random Inputs

In this case Eq 10 simplifies to

$$\Phi_o(\omega) = |G_1(j\omega)|^2 \sum_{k=1}^{N} \Phi_k(\omega) \qquad (11)$$

Several useful properties of Gaussian random process originally presented by Rice in Ref. 37 are presented in Table II. Table entries are given in terms of both the autocorrelation function evaluated at $\tau = 0$, i.e., $R(0)$, and the spectral density.

2. Probabilistic Characteristics of Random Inputs

Most random command input data are well approximated by the Gaussian probability density function. This is evidenced by the data of this report. With a single Gaussian random input and a linear transfer characteristic (see Fig. 17), the output will also be Gaussian.

The probability distribution of an input which is the sum of more than one random component can be obtained with the characteristic function (Ref. 38). The characteristic function, $C_y(\xi)$, for a random variable, $y(t)$, is given by the Fourier transform of the probability density function, i.e.,

$$C_y(\xi) = \int_{-\infty}^{\infty} p(y) e^{i\xi y} dy \qquad (12)$$

where $p(y)$ is the probability density function of $y(t)$. Now, the characteristic function for the sum of the random components is the product of the component characteristic functions. Under suitable conditions this can be inverse-Fourier-transformed to obtain the probability distribution of the sum of components.

The probability distribution of the product or quotient of more than one random variable can be obtained using the Mellin transform (Ref. 39). For one-sided probability density functions [i.e., $p(y) = 0$, $y < 0$] the Mellin transform is defined as

$$P(\xi) = \int_0^{\infty} y^{\xi-1} p(y)\, dy \qquad (13)$$

TABLE II

PROPERTIES OF GAUSSIAN INPUTS

[Note: $R''(0) = (d^2/d\tau^2)R(\tau)$ at $\tau = 0$; etc.]

PROPERTY	AUTOCORRELATION	SPECTRUM
Mean square	$R(0)$	$2\int_0^\infty \Phi(\omega)\, d\omega$
Axis crossings per second	$\frac{1}{\pi}\left[-\frac{R''(0)}{R(0)}\right]^{1/2}$	$\frac{1}{\pi}\left[\frac{\int_0^\infty \omega^2\Phi(\omega)\, d\omega}{\int_0^\infty \Phi(\omega)\, d\omega}\right]^{1/2}$
Maxima per second	$\frac{1}{2\pi}\left[-\frac{R''''(0)}{R''(0)}\right]^{1/2}$	$\frac{1}{2\pi}\left[\frac{\int_0^\infty \omega^4\Phi(\omega)\, d\omega}{\int_0^\infty \omega^2\Phi(\omega)\, d\omega}\right]^{1/2}$
Positive axis crossings of y_1 per second — — — — — — Also, maxima $> y_1$ when $y_1 >> \sigma$	$\frac{e^{-y_1^2/2R(0)}}{2\pi}\left[-\frac{R''(0)}{R(0)}\right]^{1/2}$	$\frac{e^{-y_1^2/2\sigma^2}}{2\pi}\left[\frac{\int_0^\infty \omega^2\Phi(\omega)\, d\omega}{\int_0^\infty \Phi(\omega)\, d\omega}\right]^{1/2}$

The transform, $P_3(\xi)$, of the product of two random variables, y_1 and y_2, is given by

$$P_3(\xi) = P_1(\xi)P_2(\xi) \qquad (14)$$

The probability distribution of the product results from the inverse transform of $P_3(\xi)$ using appropriate transform tables (e.g., Refs. 40 and 41). The definition of Eq 13 can be extended to two-sided distributions.

3. Deterministic Inputs

Some command inputs have a signal waveform which is fully defined in time. The Laplace transform of these inputs (or an approximation thereto) contains all the information about the input, and can be used to study controller–vehicle response characteristics.

A good example of a deterministic input is the overflight interference in the localizer signal discussed in Appendix B. The actual waveform could be approximated by a series of ramps or perhaps a decaying sinusoid to permit Laplace transformation. Other examples are pilot-generated impulses, steps, and ramps frequently used during maneuvering flight.

Extensive tables of Laplace transforms are given in Refs. 40 and 42. A compilation of dynamic performance criteria for deterministic inputs is given in Ref. 34.

C. APPROXIMATION OF RANDOM INPUT BY SUM OF SINUSOIDS

It is frequently advantageous to approximate a random input by a more useful deterministic form. One powerful approach is to use a sum of sinusoids with random phase which is random-appearing and equivalent in some way. A sum of sinusoids can be made arbitrarily equivalent to a finite sample of random data as measured by the following factors:

1. Effective number of degrees of freedom
2. Mean and mean-squared amplitudes
3. Shape of the probability density function

The approximation will not be equivalent to the random sample in terms of higher order moments of the probability distribution.

The sum of sinusoids for real, positive frequencies can take the form

$$y(t) = \sum_{k=0}^{N} A_k \cos (\omega_k t + \varphi_k) \tag{15}$$

Equation 15 approaches a Gaussian distribution for uniformly distributed φ_k, noncommensurate ω_k, and arbitrary A_k if the number of terms is sufficiently large. The convergence is more rapid if the A_k are of the same amplitude.

The autocorrelation function for y(t) is obtained by substituting Eq 15 into Eq 3 and performing the indicated manipulations.

$$R(\tau) = \sum_{k=0}^{N} \frac{A_k^2}{2} \cos \omega_k \tau \tag{16}$$

The spectral density is the most useful form in the approximation process. It is obtained by substituting Eq 16 into Eq 5 and integrating, i.e.,

$$\Phi(\omega) = \sum_{k=0}^{N} \frac{A_k^2}{4} \delta(\omega - \omega_k) \tag{17}$$

It is defined only over positive frequencies according to Eq 5. The spectral density is seen to be discrete, composed of Dirac delta functions at the frequencies of the sinusoidal components in y(t).

The approximation or "fitting" process is relatively straightforward. Consider the typical data spectrum of Fig. 20. Amplitudes, A_k,

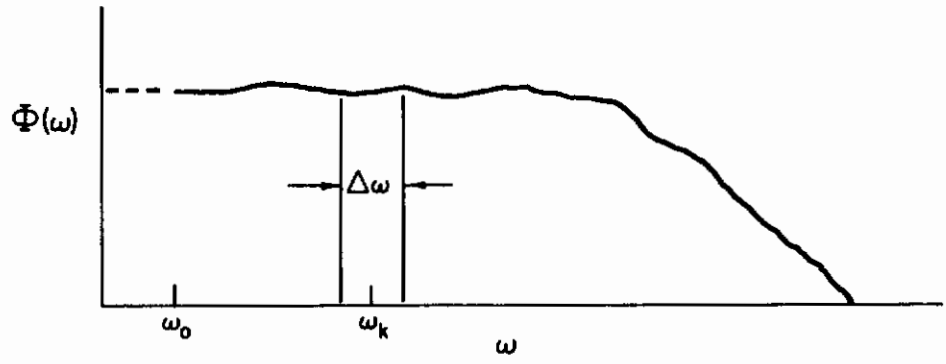

Figure 20. Typical Spectrum

and frequency separation, $\Delta\omega = \omega_{k+1} - \omega_k$, of the component sinusoids must be determined. For data having a finite run length, T, there is some minimum frequency, ω_o, below which the spectrum is undefined, i.e.,

$$\omega_o = 2\pi f_o = \frac{2\pi}{T} \tag{18}$$

This minimum frequency defines the minimum frequency separation between components, i.e.,

$$\Delta\omega = \omega_o \tag{19}$$

Integer multiples of this frequency separation can be used ($\Delta\omega = 2n\pi/T$, $n \geq 2$). Noninteger multiples can be used, but frequency separations of the order given in Eq 20,

$$\Delta\omega = \frac{\pi(2n + 3)}{2T} \quad ; \quad n = 0, 1, 2, \cdots \tag{20}$$

should be avoided, at least for $n < 4$. This will ensure that the cross-correlation between any two components is zero.

The amplitude, $A_k^2/4$, of the delta function at ω_k is proportional to the power in the spectral strip with width $\Delta\omega$ (see Fig. 20). The final scaling is accomplished to make the integral of the spectral comb equal to that of the data spectrum. If unequal widths are used (e.g., equal intervals on a log scale might be used), then the amplitudes will have to be adjusted inversely with the widths to preserve the power in the strips. Care should be taken to place components at spectral peaks. Components in the attenuated region of Fig. 20 at higher frequency have little effect, and may be deleted above a certain frequency.

The resultant "fit" should have enough components to be reasonably Gaussian. A minimum of five to eight sinusoids of roughly equal amplitude is adequate in practice. More are required if the amplitudes are nonequal. The component frequencies should be checked to insure that they are nonharmonic.

Advantages of this approximation technique include the ability to

1. Approximate any power spectral density
2. Know the mean and mean-squared amplitudes
3. Control the degree of apparent randomness
4. Obtain "exact" answers with only one run and in a computable minimum run length (finite time)
5. Have each frequency component of a random time function in a form suitable for separate use
6. Perform the analog or digital simulation of a random process, without using a noise generator

Disadvantages are that

1. Higher order probability distributions are not Gaussian
2. The maximum possible amplitude is fixed by the sum of the amplitudes of the components
3. The data should be in power spectral density form, which may require data reduction
4. Relative attenuation of any of the component sinusoids due to filtering will tend to make the resultant signal less Gaussian

SECTION VI

RECOMMENDATIONS

A. GENERAL

1. Preferred Data Forms

The most useful descriptors of random inputs are the power spectral density and the probability distribution. Conditions and techniques used in the data collection and reduction are essential to a proper evaluation. These might include, for example, run length, degrees of freedom, sampling interval, and adequate definition of the mathematical relations (see Ref. 43). Peak amplitude over a finite time is another useful statistic.

Deterministic inputs are fully defined by their waveform. The expected value and range of variation in key parameters are useful. Examples include possible perturbations in amplitude, duration, period, and envelope of the input signal.

2. Distribution

Currently, the only way to distribute and interchange data between sources and flight control designers is through publication by the originator. A concurrent effort under this contract is studying the problem of flight control data interchange, but implementation is not currently contemplated. The need for the data is apparent. The solution for the immediate future remains publication (preferably unclassified) by the originator, with bibliographic "descriptors" indicative of the data content.

B. AREAS OF DATA NEED

Certain data included in this report are either incomplete or not in a readily usable format. As a result, acquisition of the following data might be appropriate (not necessarily in order of importance):

1. ILS glide path spectral densities and probability distributions over the relatively stationary regions.
2. More ILS directional localizer spectral densities. The three currently available may not be representative of those in widespread use.
3. More pilot remnant data. Reduction of existing remnant data would complete the picture in this vital area.
4. More automatic landing system angle noise data. Representative results for systems in current use are needed.

Command input data should also be available for design of flight control systems in the areas of

1. Low altitude radio altimetry, particularly during landing or terrain following
2. Booster control
3. Air-to-air gunnery

REFERENCES

1. Hart, J. E., L. A. Adkins, and L. L. Lacau, Stochastic Disturbance Data for Flight Control Systems Analysis, ASD-TDR-62-347, Sept. 1962.

2. Metz, H. I., "A Study of Instrument Approach Systems in the United States," IRE Trans., Vol. ANE-6, No. 2, June 1959, pp. 78–84.

3. Jackson, W. E., "Improvement on the Instrument Landing System," IRE Trans., Vol. ANE-6, No. 2, June 1959, pp. 85–94.

4. Iden, F. W., "Glide-Slope Antenna Arrays for Use Under Adverse Siting Conditions," IRE Trans., Vol. ANE-6, No. 2, June 1959, pp. 100–111.

5. Hansford, R. F., ed., Radio Aids to Civil Aviation, Heywood and Company, Ltd., London, 1960.

6. Standard Performance Criteria for Autopilot/Coupler Equipment, Radio Technical Commission for Aeronautics, Paper 131-61/SC79-58 (Fourth Draft), Aug. 1961.

7. Gill, F. R., M. E. Smith, and J. D. Asteraki, An Experimental Assessment of the Stability of the Course Line of an I.L.S. Localiser Ground Equipment, Royal Aircraft Estab., Tech. Note BL. 54 (DDC AD-406 047), Jan. 1963.

8. Hollm, E. R., N. J. Proferes, and A. B. Winick, Capability of the Directional Localizer as a Source of Azimuthal Guidance for Landing, Paper presented at FAA Research and Development Symposium, Atlantic City, Apr. 1961.

9. Doniger, J., Analytical Study of ILS beam Characteristics, The Bendix Corp., Eclipse-Pioneer Div., Aug. 31, 1962.

10. Marschall, F. W., Standard Directional Localizer Overflight Interference, Federal Aviation Agency, July 1962.

11. Doniger, J., A Study of the Effects on Lateral Automatic Landing Performance of Overflight Interference with the Waveguide Directional Localizer, The Bendix Corp., Eclipse-Pioneer Div., Phase II, Final Report, Apr. 15, 1963.

12. Moses, K., and J. Doniger, The Analysis and Performance of All Weather Landing Systems Using ILS Data, Paper presented at the SAE Committee-18 Meeting, Phoenix, Ariz., Dec. 6–8, 1961.

13. Friedman, A., and J. Doniger, Analog Computer Study of Safe Low Approach Decision Regions and Effectiveness of Glide Path Extension Techniques, The Bendix Corp., Eclipse-Pioneer Div., Phase III Final Report, Mar. 31, 1964.

14. Chernin, M. G., Analysis of ILS Glide Slope Antennas in Operation and Under Development, National Engineering Science Co., Rept. RD-64-11 (DDC AD-435 568), Feb. 1964.

15. Cutler, B., and L. Sanders, "REGAL — An advanced Approach and Landing System," IRE Trans., Vol. ANE-6, No. 2, June 1959, pp. 135-142.

16. Automatic Landing System Study, Part II, Results of Ground Equipment and Data Transmission Studies, ASD-TR-61-114, Part II, Feb. 1962.

17. Powell, F. D., "An Automatic Landing System," IRE Trans., Vol. ANE-6, No. 2, June 1959, pp. 128-135.

18. Powell, F. D., New Developments in Automatic Landing, SAE Paper 516E, April 1962.

19. Delano, R. H., "A Theory of Target Glint or Angular Scintillation in Radar Tracking," Proc. IRE, Vol. 41, No. 2, Dec. 1953, pp. 1778-1784.

20. Muchmore, R. B., "Aircraft Scintillation Spectra," IRE Trans., Vol. AP-8, No. 2, Mar. 1960, pp. 201-212.

21. Povejsil, D. J., R. S. Raven, and P. Waterman, Airborne Radar, D. Van Nostrand Co., Inc., New York, 1961.

22. Informal communication from NOTS (R. Schwarzbach), Nov. 1965.

23. Kerr, D. E., ed., Propagation of Short Radio Waves ("MIT Radiation Lab. Series," Vol. 13), Boston Tech. Pub., Inc., Lexington, Mass., 1964.

24. Terrain-Avoidance Seminar, October 17-19, 1961, Cornell Aeronautical Lab. Rept. CAL-116, Oct. 1961. (Report CONFIDENTIAL)

25. McRuer, D., D. Graham, E. Krendel, and W. Reisener, Jr., Human Pilot Dynamics in Compensatory Systems — Theory, Models, and Experiments with Controlled Element and Forcing Function Variations, AFFDL-TR-65-15, July 1965.

26. Weir, D. H., and A. V. Phatak, Model of Human Operator Response to Step Transitions in Controlled Element Dynamics, Systems Technology, Inc., Tech. Rept. 151-1, June 1965. (Forthcoming NASA Contractor Report)

27. McRuer, D. T., and E. S. Krendel, Dynamic Response of Human Operators, WADC-TR-56-524, Oct. 1957.

28. Truxal, J. G., ed., Automatic Feedback Control System Synthesis, ("McGraw-Hill Electrical and Electronic Engineering Series"), McGraw-Hill Book Co., Inc., New York, 1955.

29. Graham, D., and D. McRuer, Analysis of Nonlinear Control Systems, John Wiley and Sons, Inc., New York, 1961.

30. McRuer, D. T., Unified Analysis of Linear Feedback Systems, ASD-TR-61-118, July 1961.

31. McRuer, D. T., and R. L. Stapleford, Sensitivity and Modal Response for Single-Loop and Multiloop Systems, ASD-TDR-62-812, Jan. 1963.

32. McRuer, D. T., I. L. Ashkenas, and H. R. Pass, Analysis of Multiloop Vehicular Control Systems, ASD-TDR-62-1014, Mar. 1964.

33. Wolkovitch, J., and R. Magdaleno, Performance Criteria for Linear Constant-Coefficient Systems with Random Inputs, ASD-TDR-62-470, Jan. 1963.

34. Wolkovitch, J., R. Magdaleno, D. McRuer, et al, Performance Criteria for Linear Constant-Coefficient Systems with Deterministic Inputs, ASD-TR-61-501, Feb. 1962.

35. Laning, J. H., Jr., and R. H. Battin, Random Processes in Automatic Control ("McGraw-Hill Series in Control Systems Engineering"), McGraw-Hill Book Co., Inc., New York, 1956.

36. Davenport, W. B., Jr., and W. L. Root, An Introduction to the Theory of Random Signals and Noise ("MIT Lincoln Lab. Publications"), McGraw-Hill Book Co., Inc., New York, 1958.

37. Wax, N., ed., Selected Papers on Noise and Stochastic Processes, Dover Publications, Inc., New York, 1954.

38. Bennett, W. R., "Methods of Solving Noise Problems," Proc. IRE, Vol. 44, No. 5, May 1956, pp. 609–638.

39. Dolan, B. A., "The Mellin Transform for Moment-Generation and for the Probability Density of Products and Quotients of Random Variables," Proc. IEEE ("Correspondence"), Vol. 52, No. 12, Dec. 1964, pp. 1745–1746.

40. Erdélyi, A., ed., Tables of Integral Transforms, Vol. I, McGraw-Hill Book Co., Inc., New York, 1954.

41. Erdélyi, A., ed., Tables of Integral Transforms, Vol. II, McGraw-Hill Book Co., Inc., New York, 1954.

42. Gardner, M. F., and J. L. Barnes, Transients in Linear Systems, John Wiley and Sons, Inc., New York, 1942.

REFERENCES (Cont'd)

43. Blackman, R. B., and J. W. Tukey, The Measurement of Power Spectra from the Point of View of Communications Engineering, Dover Publications, Inc., New York, 1958.

44. Doniger, J., Analytical Study of ILS Beam Characteristics, The Bendix Corp., Eclipse-Pioneer Div., First and Second Monthly Letter Progress Rept., November–December 1961.

45. Informal communication from Mr. J. Doniger, Bendix–Eclipse Pioneer Div., Nov. 1965.

46. Gill, F. R., and P. England, I.L.S. Localiser Feasibility Study: Progress Report on Interference from Overflying Aircraft, Royal Aircraft Estab., Tech. Note BL. 59, Feb. 1963.

47. Pelton, F. M., Advance Concepts for Terrain Avoidance (ADCON), ASD-TR-61-468, 30 Oct. 1961. (Report CONFIDENTIAL)

48. Pelton, F. M., Studies and Simulation of Terrain Avoidance Problems (ADCON II), First Quarterly Progress Rept., Cornell Aeronautical Lab. Rept. IH-1705-E-1, 1 May – 1 August 1962. (Report CONFIDENTIAL)

49. Pelton, F. M., Studies and Simulation of Terrain Avoidance Problems, Vol. II, Terrain Following Control Techniques, ASD-TDR-63-612-II, July 1963. (Report CONFIDENTIAL)

50. Jocoy, E. H., Studies and Simulation of Terrain Avoidance Problems, Vol. III, Effects of Noise and Target Scintillation on Monopulse Radar, ASD-TDR-63-612-III, Jan. 1964. (Report CONFIDENTIAL)

51. Schwartz, E. C., ADLAT — Terrain Avoidance Techniques Evaluation, AL-TDR-64-145, Aug. 1964. (Report CONFIDENTIAL)

52. Informal communication from Cornell Aeronautical Lab. (F. M. Pelton), Jan. 1965.

APPENDIX A

ANALYSIS OF ILS LOCALIZER POWER SPECTRAL DENSITY DATA

Irregularities occur in the ILS localizer course structure due to reflections from both the terrain and physical structures along the approach path. Thus, if an aircraft were to follow the ILS receiver output signal with zero error, it would still exhibit lateral excursions about the projected runway centerline. The nature of these course line irregularities as a noise component in the FCS command input is the subject of this appendix.

BASIC DATA

The basic data were obtained by the FAA and were published by Bendix in Ref. 9. The course line structure was obtained from the outer marker to the runway threshold for 24 localizer facilities throughout the U. S. The data-generation procedure consisted of flying the localizer and recording the receiver output signal on board the aircraft, as well as the deviation of the aircraft about the extended centerline with a theodolite. The received errors and the inertial path of the aircraft from the theodolite were then combined to obtain the course line structure. The result is one record for each facility giving the deviation in microamperes of the transmitted course about the ideal course along the centerline. The records are for one run and do not represent averages. The aircraft tracking accuracy was on the order of ±2.5 ft, and the theodolite sampling interval was approximately 1 sec (Ref. 9). The receiver output was recorded continuously.

The on-board measurements appear to have been made at the output of a standard localizer receiver (Ref. 9). The receiver output is low-pass filtered with a time constant of approximately 0.5 sec (Ref. 8). Thus, the true course noise will be attenuated in the data above a frequency of 2 rad/sec.

Twelve of the 24 localizer facilities were analyzed in detail in Ref. 9, and the theodolite-corrected course line deviations are presented

in Fig. 21 . These twelve were selected because statistical analysis showed that each was sufficiently self-stationary to be considered a finite sample of a corresponding stationary random process. This stationarity premise is essential to subsequent analyses. Tests of normality were also made and the records were found to be Gaussian. This is demonstrated in the histograms of Fig. 22 . The DC biases evident in Fig. 22 are relatively unimportant, since they can be removed by adjusting the transmitter. It is the variance about the mean that causes a noisy signal.

BENDIX EP ANALYSIS

The objective of the data analysis in Ref. 9 was to correlate lateral dispersions of a test aircraft in flight and localizer spectral parameters. If successful, this would allow use of the spectrum as an acceptability criterion. This objective was not reached completely; however, the derived localizer spectra represent a useful by-product of the study.

The derivation of power spectra from the recordings of Fig. 21 is detailed in Refs. 12 and 44. The deviations as a function of distance in Fig. 21 become time histories for a given aircraft velocity. The data reduction procedure for these time histories is summarized in the block diagram of Fig. 23 adapted from Ref. 12. The finite time run was recorded on a continuous loop as shown in Fig. 23 . The spectral results were obtained by bandpass filtering. The means, mean squares, and frequency functions were obtained also.

The "spectra" in Ref. 9 are plots of power (microamps squared) versus frequency, not power density (microamps squared per cps). Thus, the integral of a Ref. 9 spectrum does not yield the corresponding mean square. Consequently, the data were reanalyzed to obtain spectral densities for analytical use as an FCS command input.

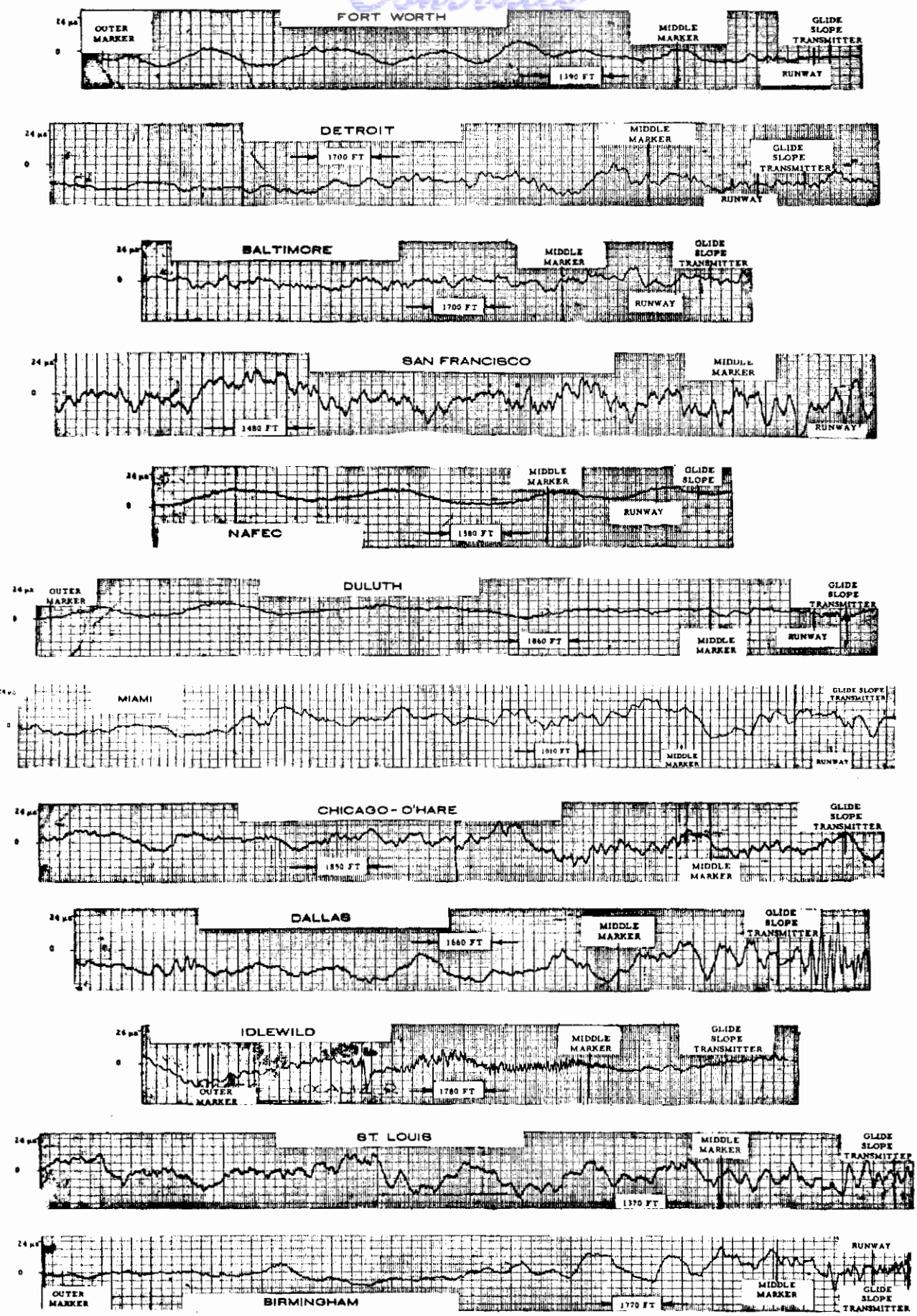

Figure 21 . Theodolite-Corrected Localizer Data (Ref. 9)

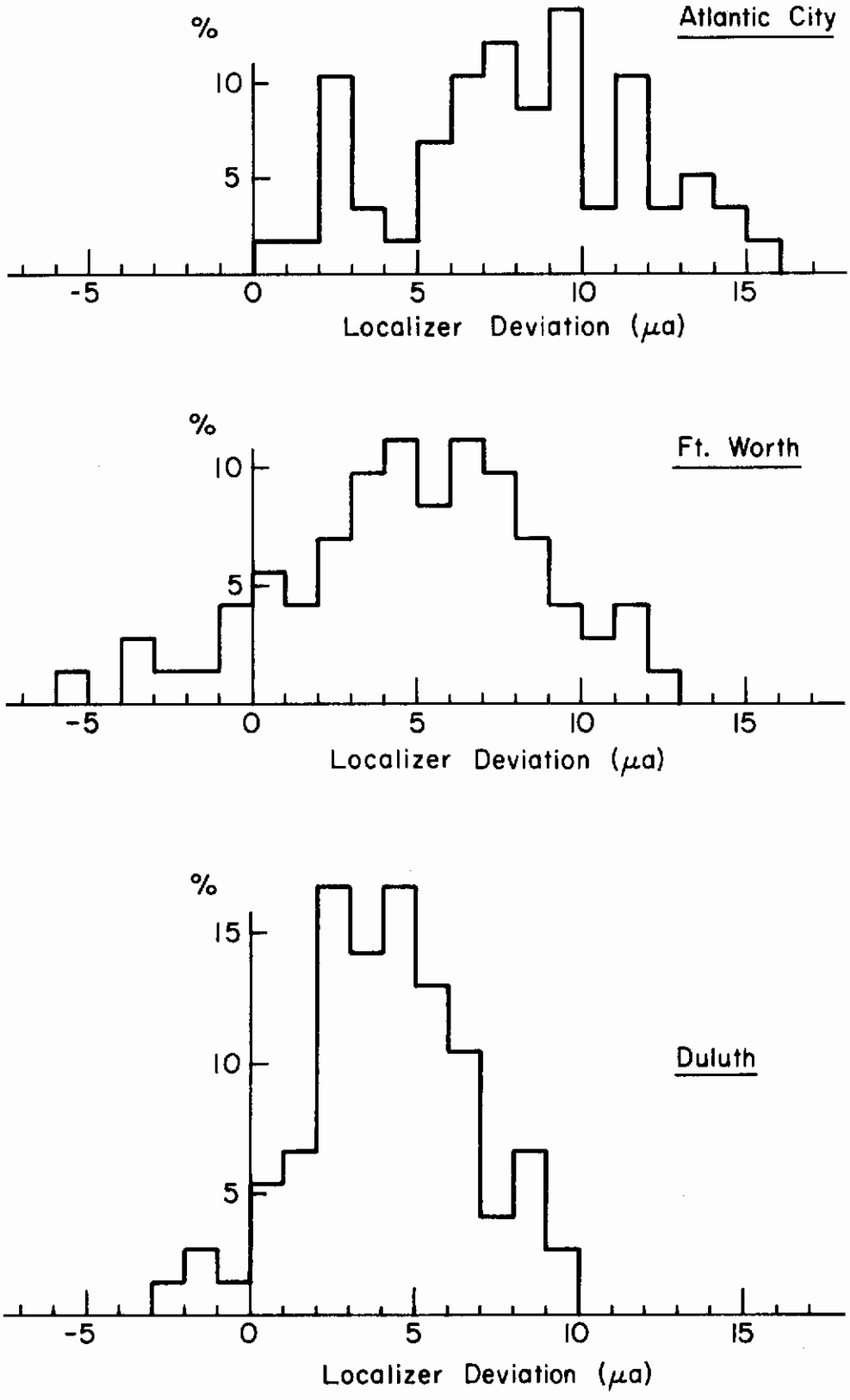

Figure 22. Deviation Amplitude Histograms for Directional Localizers

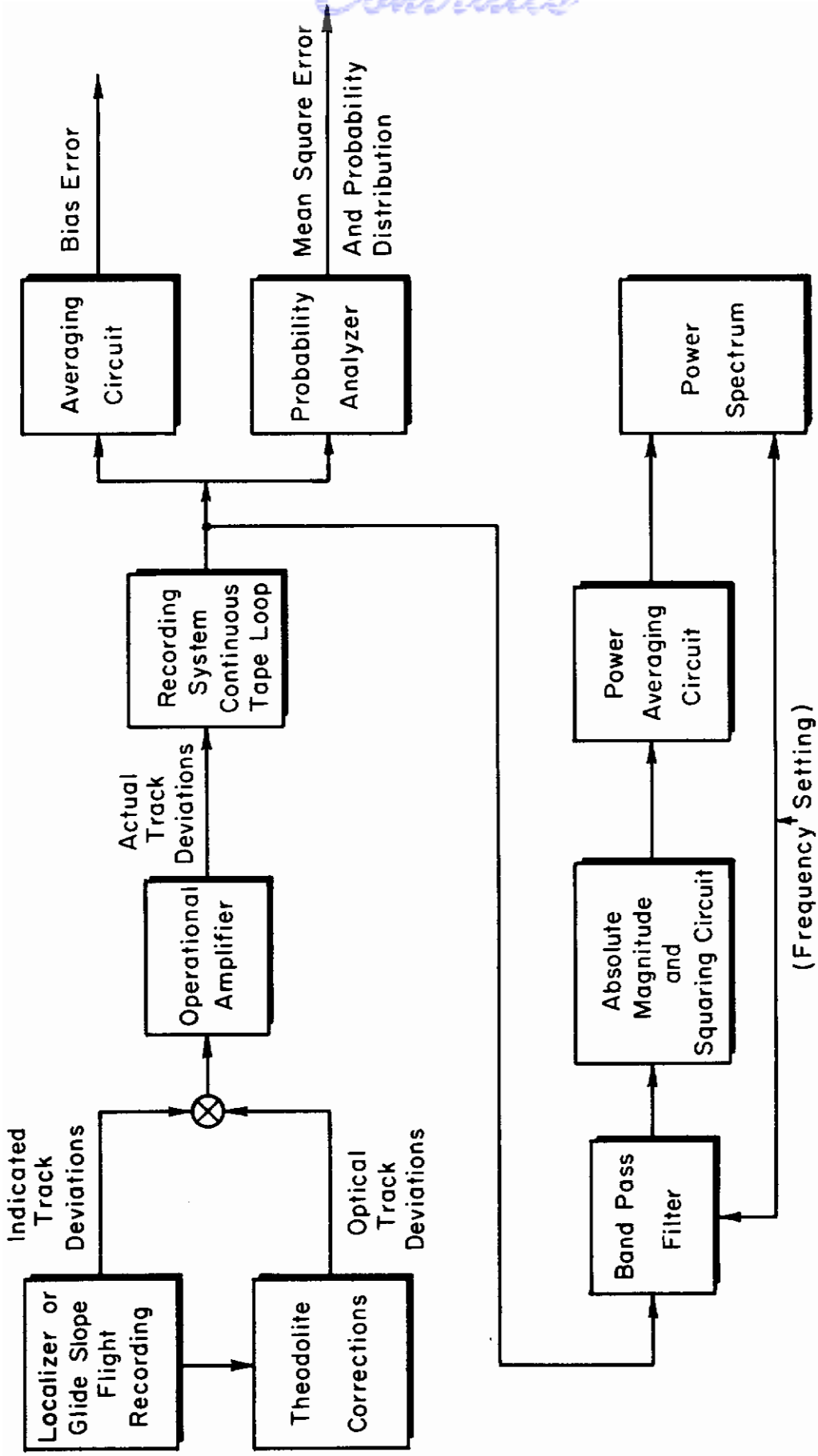

Figure 23 Block Diagram of ILS Data Reduction Procedure (Ref. 12)

REANALYSIS OF DATA

The means and mean squares (or variances) were checked against the Fig. 21 data for all twelve localizer facilities. Discrepancies occurred in two cases [Miami and Atlantic City (NAFEC)] and new values of the mean and variance were computed for these facilities from the course deviation records. These were used in subsequent derivation of the power spectral densities.

COMPUTATION OF SPECTRAL DENSITY

The "power spectra" of Ref. 9 do not have the power spectral density form. In effect, they have not been divided by the effective filter bandwidth of Fig. 22. The filter bandwidth is not available at this time, so the correction cannot be applied directly. However, it was the same at all frequencies (Ref. 45), so the power plots of Ref. 9 have the same shape in amplitude as the desired spectral density. In this case, knowledge of the variance, σ^2, can be used to adjust the ordinates and obtain the spectral densities of Figs. 24 and 25.

The conversion to density form is accomplished by computing the effective filter bandwidth, $\Delta\omega$, for each facility knowing the σ^2 and the measured area (integral) of the power plots of Ref. 9. The Ref. 9 plots have power, $P(f)$, in microamperes squared versus frequency, f, in cycles per second. Letting Δf be the effective filter bandwidth in cycles per second, the power spectral density is defined as

$$\Phi(f) = \frac{P(f)}{\Delta f} \tag{21}$$

In terms of frequency, ω, in radians per second this is equivalently

$$\Phi(\omega) = \frac{P(\omega)}{\Delta\omega} \tag{22}$$

In terms of the spectral density, $\Phi(f)$, the mean square or variance is

$$\sigma^2 = 2\int_0^\infty \Phi(f)\, df \tag{23}$$

It is desired to find $\Delta\omega = 2\pi\Delta f$. Substituting Eq 21 into Eq 23 yields

$$\sigma^2 = 2\int_0^\infty \frac{P(f)}{\Delta f}\, df$$

$$= 2\int_0^\infty \frac{2\pi P(f)}{\Delta\omega}\, df \qquad (24)$$

Recognizing that $\Delta\omega$ is a constant (for any one facility), Eq 24 becomes

$$\sigma^2 = \frac{4\pi}{\Delta\omega}\int_0^\infty P(f)\, df \qquad (25)$$

Solving Eq 25 for $\Delta\omega$,

$$\Delta\omega = \frac{4\pi}{\sigma^2}\int_0^\infty P(f)\, df \qquad (26)$$

The variances, σ^2, are given in Ref. 9. The integration in Eq 26 was accomplished graphically by replotting the power plots of Ref. 9 on linear scales. The computation of $\Delta\omega$ using Eq 26 is summarized in Table III.

Ideally, the $\Delta\omega$ values in Table III would be the same. Variations are probably due to several reasons. There is uncertainty in σ^2 when the average deviation (DC bias) is large and σ^2 is small. Some facilities had significant power at very low frequencies, resulting in inaccuracies in the integral of $P(f)\,df$. The noise level in the recordings and reduction at high frequency is not known, and may bias the integration of $P(f)\,df$ at high frequencies.

SPECTRAL DENSITY RESULTS

The power plots of Ref. 12 were converted to spectral densities using Eq 22 and the results of Table III. These spectral densities satisfy the relation

$$\sigma^2 = 2\int_0^\infty \Phi(\omega)\, d\omega \qquad (27)$$

TABLE III

COMPUTATION OF SPECTRAL DENSITY

FACILITY	$\int_0^\infty P(f)\,df$ (μa^2-cps)	σ^2 (μa^2)	$\Delta\omega = \frac{4\pi}{\sigma^2}\int_0^\infty P(f)\,df$ (rad/sec)
Fort Worth.....	0.0684	26.0	0.0332
Detroit.....	0.0607	42.3	0.0180
Baltimore.....	0.106	22.1	0.0603
San Francisco.....	0.226	62.0	0.0458
Atlantic City (NAFEC)...	0.0186	13.4*	0.0174
Duluth.....	0.020	3.6	0.0695
Miami.....	0.202	40.0*	0.0635
Chicago (O'Hare).....	0.0677	33.7	0.0252
Dallas.....	0.0650	29.0	0.0282
New York (Idlewild).....	0.0628	22.0	0.0358
St. Louis.....	0.1214	48.0	0.0318
Birmingham.....	0.1802	43.0	0.0527

*Corrected value derived from course record, Fig. 21

Nine of the facilities employed conventional localizer antenna arrays, and their spectral densities are plotted in Fig. 24. Three of the facilities used the directional localizer with a 117-ft slotted waveguide antenna. The resultant spectral densities are given in Fig. 25. The ordinates in Figs. 24 and 25 are given in power db, obtained by a 10 $\log_{10}$ conversion.

Plots of the average spectral densities for both the conventional and directional localizers are given in Section II-B of the report. One-sigma, $\pm\sigma$, limits due to interfacility variation are given for the conventional localizers, and the range is given for the directional localizers.

ERROR DISCUSSION

Another potential source of error in the spectral densities is due to the decreased number of degrees of freedom in finite run length data. For a given run length (in time) there is a frequency below which the data have little meaning because of truncation errors.

Typical run lengths appear to be about 100 sec, based on Fig. 21 and a nominal approach speed. If the tape loops of Fig. 23 had been processed once in real time, only a few degrees of freedom would have resulted. However, each tape loop was scanned over a period of several hours (Ref. 45) to obtain a more satisfactory number of degrees of freedom.

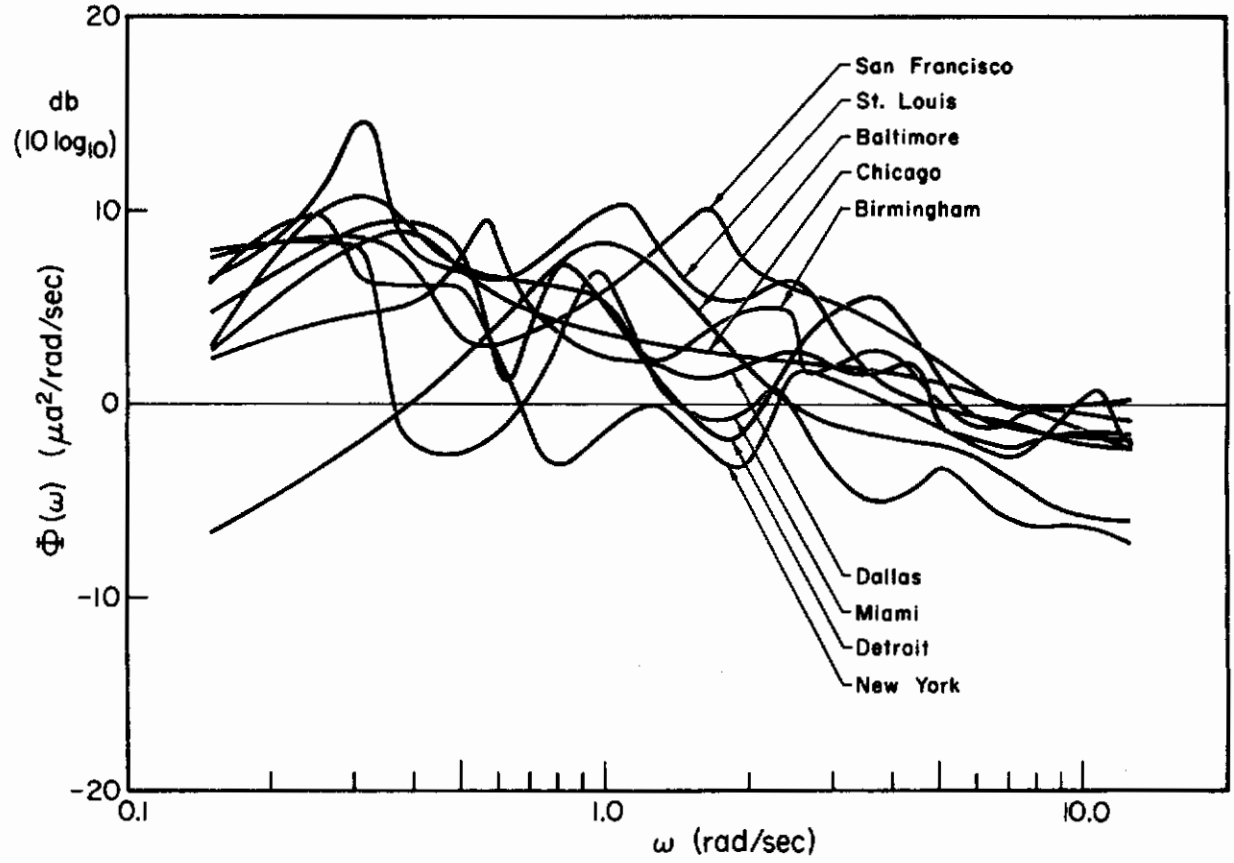

Figure 24. Power Spectral Densities for Conventional Localizers

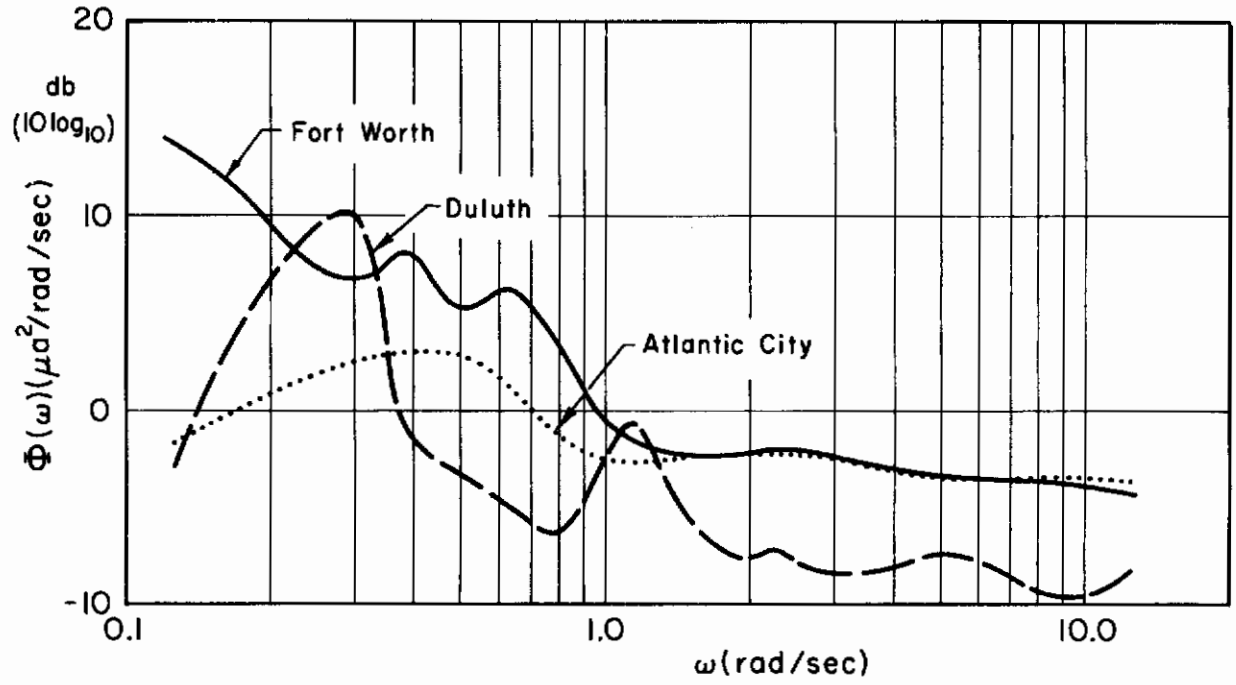

Figure 25. Power Spectral Densities for Directional Localizers

APPENDIX B

ANALYSIS OF LOCALIZER OVERFLIGHT INTERFERENCE DATA

Disturbance deviations or interference in the localizer receiver signal may occur when another aircraft is above and ahead of the landing aircraft. The interference may become significant during the last 10 to 20 sec before touchdown when the landing aircraft is below the beam, while the overflying aircraft is in a relatively strong signal region.

DATA SOURCES

Two studies have resulted in overflight interference data. Results of a theoretical study by RAE-Bedford are given in Ref. 46 for a conventional ILS localizer. The FAA conducted an experimental program reported in Refs. 8 and 10 with a directional (117-ft slotted waveguide) ILS localizer. Further analysis of the FAA data accomplished by Bendix Corporation is reported in Ref. 11. The FAA data are reported herein because the data and analyses of Refs. 8, 10, and 11 are more extensive, and because they refer to the more topical directional localizer. The results of Ref. 46 differ somewhat from those of the FAA study, primarily because of the difference in the antennas.

INTERFERENCE VOLUME

An interference volume is defined above the approach and landing area as that region within which the presence of an overflying aircraft can cause interference at the landing aircraft. Interference is defined in Ref. 10 (for example) as a disturbance deviation which has a peak amplitude in excess of 10 μa, has a principal frequency content of less than 1 cps, and has a duration in excess of 0.5 sec. A typical interference volume based on this criterion is sketched in Fig. 26, adapted from Fig. 5 of Ref. 11.

Several parameters define the boundaries of the volume for any given interference situation. Principal among these are (from Ref. 10):

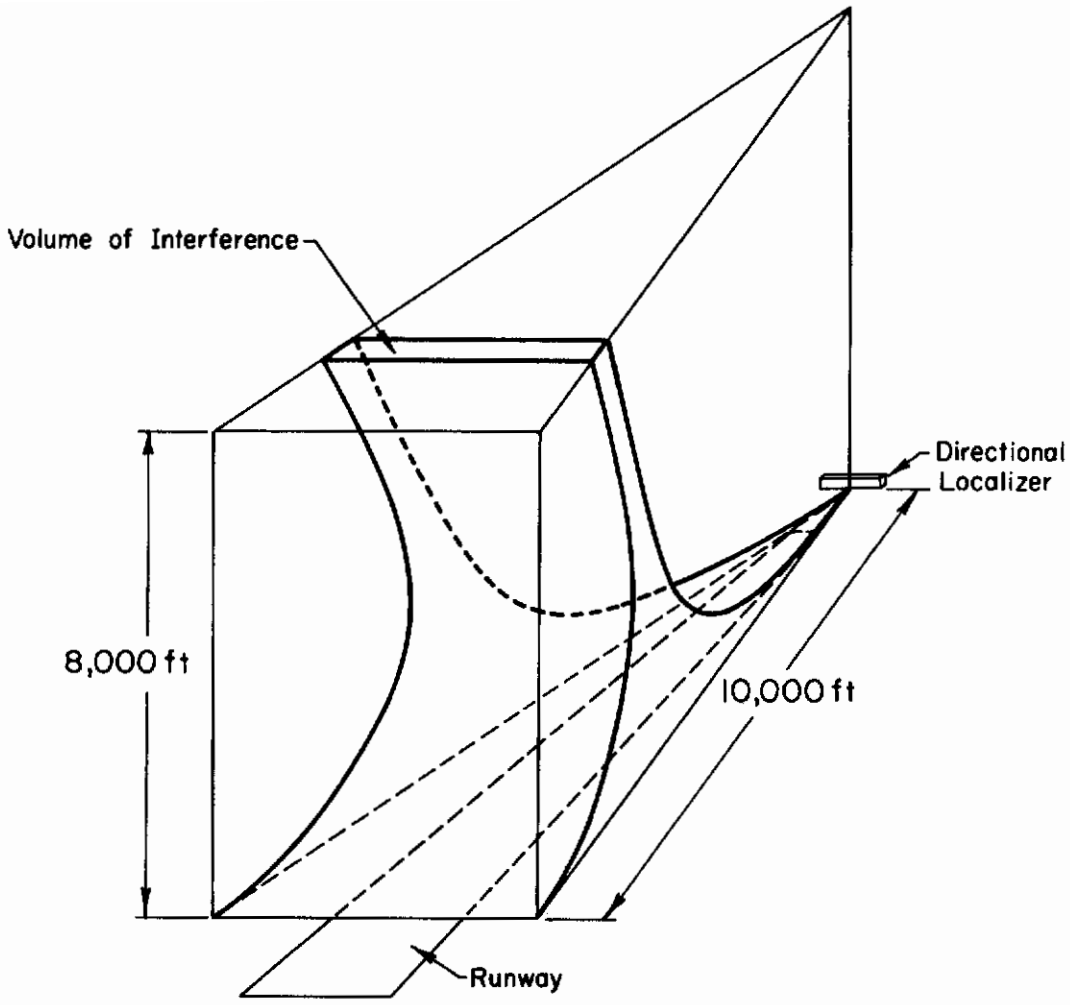

Figure 26. Typical Interference Volume (Ref. 11)

1. The interference or disturbance deviation criterion
2. Relative positions of the interfering and landing aircraft
3. Velocities of the two aircraft
4. Reflective cross section of the interfering aircraft
5. Antenna beam structure

It is obvious that definitive results cannot be presented for all realistic combinations of these variables. Consequently, the data available and those which are presented herein only define some of the important limiting cases, and tend to suggest typical interference characteristics (amplitude, frequency content, and duration).

DEVIATION AMPLITUDE

The bulk of the overflight interference data consists of deviation amplitudes (in microamperes) of the localizer receiver output signal. The localizer receiver output filter has a time constant of about 0.5 sec (Refs. 8 and 10), so the higher frequency content of all the succeeding interference data is suppressed. The amplitudes are given as a function of interfering aircraft position and velocity within the interference volume. The reflective cross section and beam structure are assumed constant, and the landing aircraft receiver is at low altitude near the runway threshold.

FLIGHT PATHS PERPENDICULAR TO RUNWAY CENTERLINE

Amplitude deviations due to interfering aircraft flight paths perpendicular to the runway at various distances from the transmitting localizer antenna are given in Ref. 10. The paths are shown in Fig. 27.

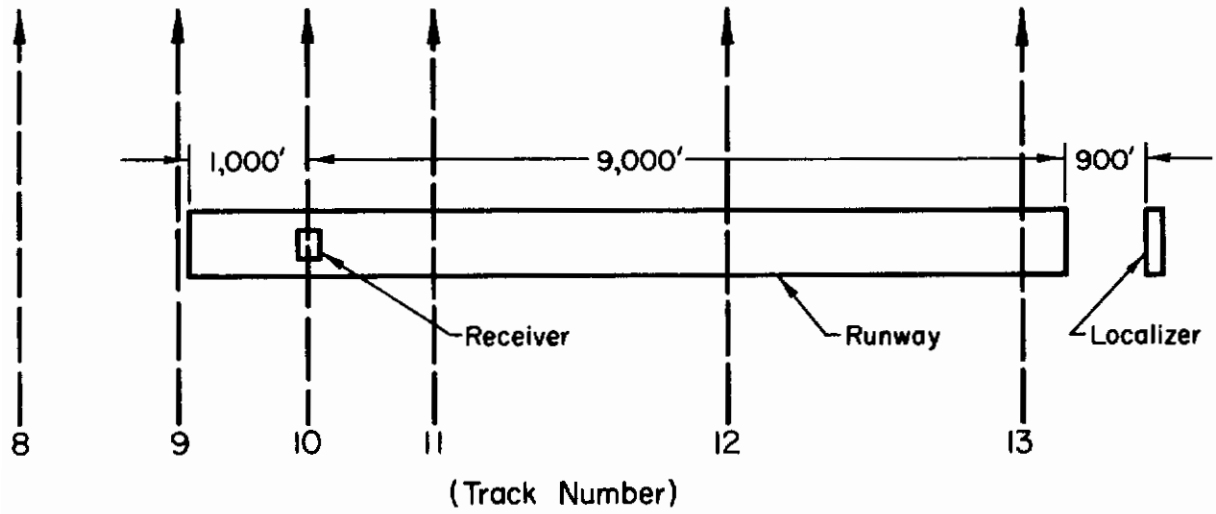

Figure 27. Paths of Overflying Aircraft (Fig. 4, Ref. 10)

The tests were static in nature, and the receiver antenna was fixed at a height of 10 ft as shown. The interference flight paths were flown with a DC-3 at an altitude of 2000 ft and a speed of 150 knots. The envelope of amplitude deviations is given in Fig. 28 as a function of aircraft azimuth from the receiver. As noted, the receiver output is filtered ($T \doteq 0.5$ sec) so only the low frequency envelope is presented in Fig. 28.

Note: Receiver antenna height = 10 ft
Overflying aircraft height = 2,000 ft

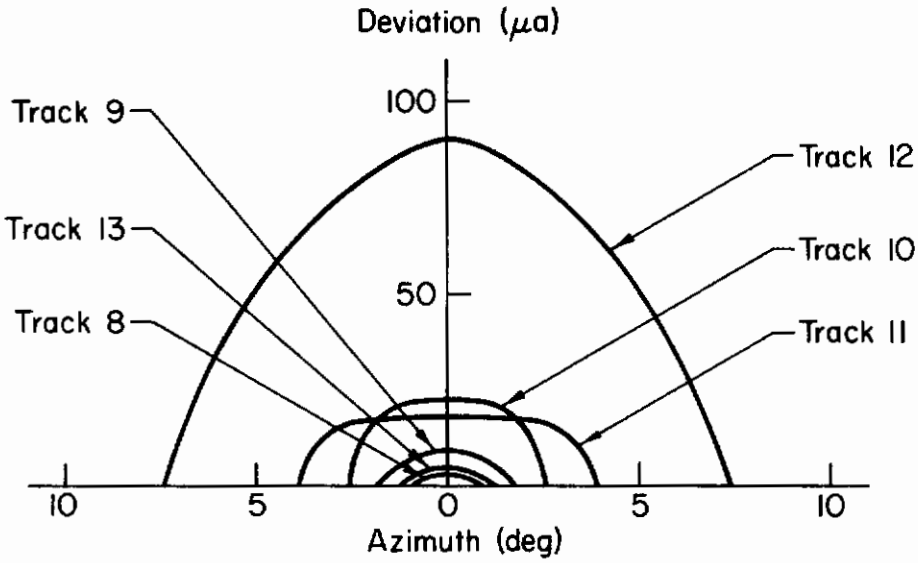

Figure 28. Amplitude Deviation Envelopes for Perpendicular Flight Paths (Fig. 6, Ref. 10)

FLIGHT PATHS ALONG THE RUNWAY CENTERLINE

The effect of interference flight paths along the runway centerline was investigated also in Ref. 10. The receiver antenna was set at heights of 10, 20, and 30 ft at the same position shown in Fig. 27. Flights were made along the runway centerline with a DC-3 at three altitudes. The peak deviations during the flights for the different antenna heights were recorded, and these are plotted in Fig. 29. The sharp reduction in disturbance deviation amplitude with increasing antenna height is readily seen. Since the height of the antenna on transport aircraft in the horizontal ground position is in the range of 20 to 30 ft (Ref. 8), the larger deviations may be unrealizable in practice.

The variation of maximum deviation with interfering aircraft altitude is shown in Fig. 30. The flight paths were along the runway centerline. The receiver antenna was fixed at a height of 10 ft at the position shown in Fig. 27. The peaking effect near an altitude of 4500 ft seen in the Fig. 29 data is shown in Fig. 30 also. As noted above, an antenna height of only 10 ft may be unrealistically low, even for an aircraft that is on the runway.

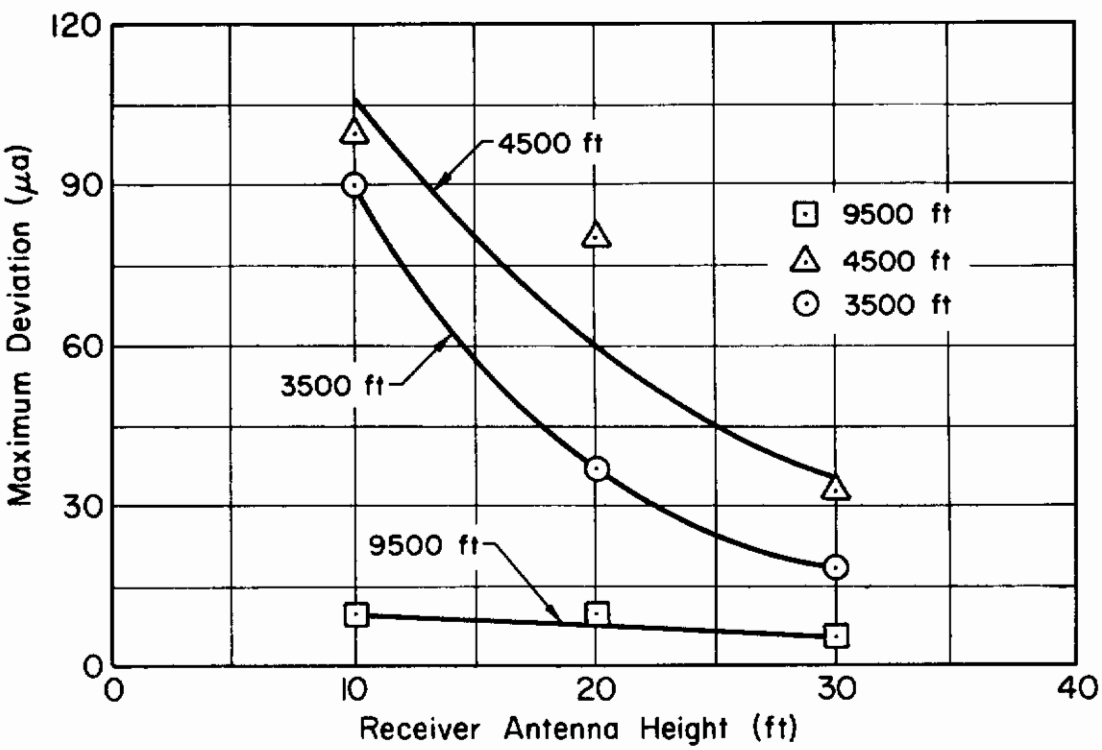

Figure 29. Maximum Deviations for Centerline Flight Paths (Fig. 9, Ref. 10)

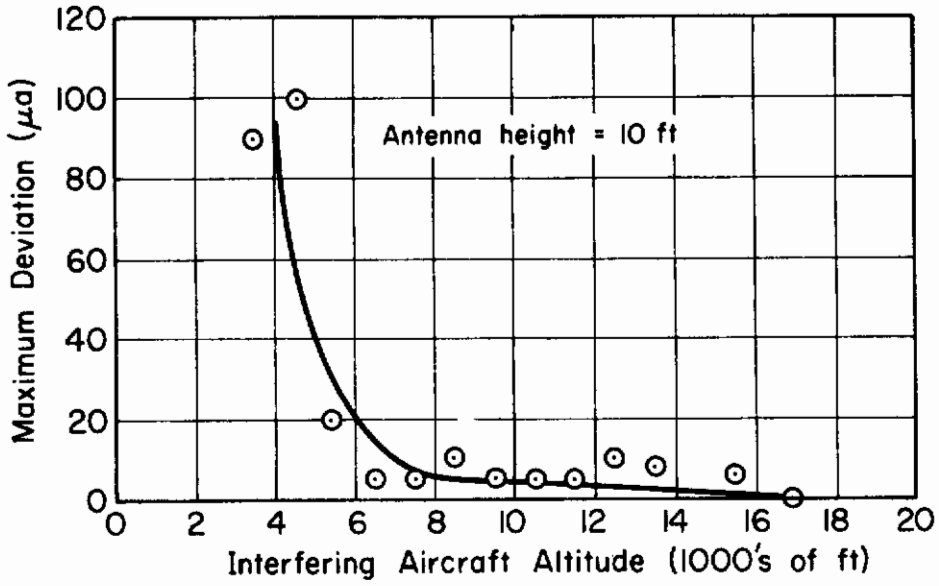

Figure 30. Maximum Deviation Versus Altitude (Fig. 10, Ref. 10)

The largest disturbance deviations are probably caused by an aircraft flying over the localizer at takeoff altitudes at the same time the landing aircraft is at the runway threshold (Ref. 10). A good example of the amplitude and duration of this type of interference is given by Run 2 of Test 5, Ref. 10, shown in Fig. 31 . The data in Fig. 31 were recorded at the receiver output of the landing aircraft under dynamic conditions.

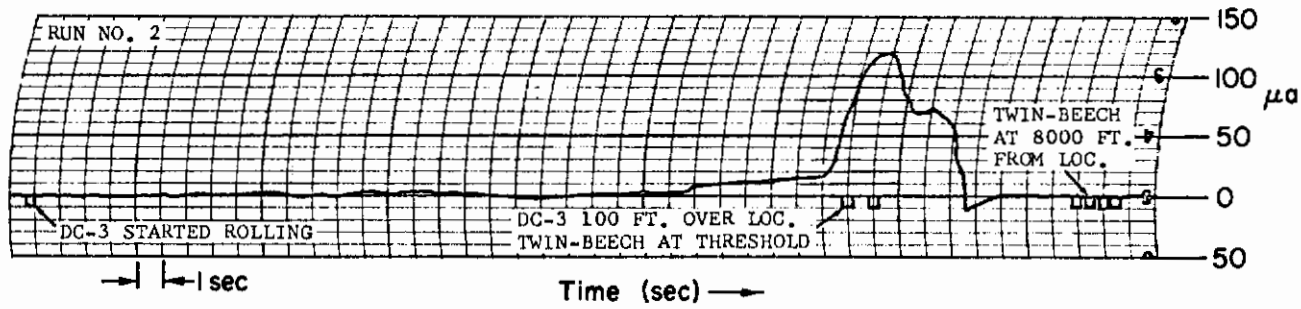

Figure 31. Deviation Due to Takeoff Over Antenna
(Fig. 19, Ref. 10)

In Fig. 31 the DC-3 was at an altitude of 100 ft over the directional localizer when the landing aircraft was less than 50 ft above the runway at the threshold. Other data in Ref. 10 show that the perturbations are significantly smaller when the takeoff aircraft and landing aircraft are higher. Air traffic control procedures should prevent the occurrence of this particular interference situation under normal conditions because of its known severity.

IDEALIZATION OF OVERFLIGHT DISTURBANCES

Signal deviations due to overflying aircraft are deterministic waveforms of short duration. This is in sharp contrast to the majority of FCS command inputs (either intentional or undesired) which persist for relatively long periods and can frequently be approximated as a sample of a stationary random process. Consequently, spectral techniques are not applicable and deterministic descriptors should be used for analytic or simulation studies.

An extensive series of analog studies are reported in Ref. 11. The simulated interference inputs to the FCS used in these studies are both

pertinent and realistic because they are based on a considerable familiarity with the FAA data summarized in Refs. 8 and 10.

The frequency content of the receiver output was assumed to vary linearly with duration, T, as shown in Fig. 32 (adapted from Fig. 25 of Ref. 11). Durations, T, from 5 to 40 sec were simulated; however, values around 5 sec appear to be the most representative (Ref. 8).

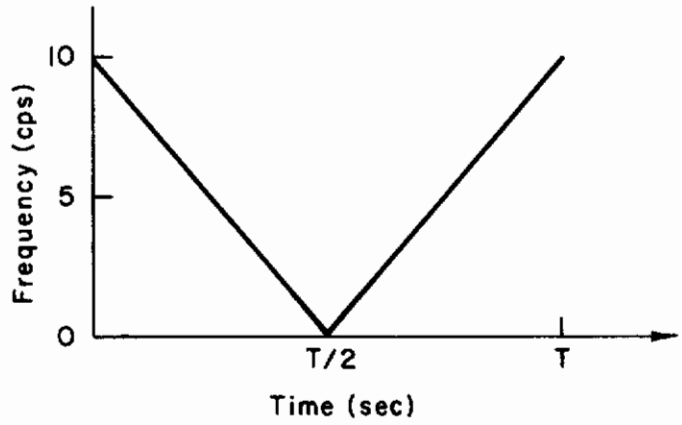

Figure 32. Idealized Disturbance Frequency Variation

The envelope of amplitude deviations was assumed to vary with frequency as shown in Fig. 33 (adapted from Fig. 25 of Ref. 11).

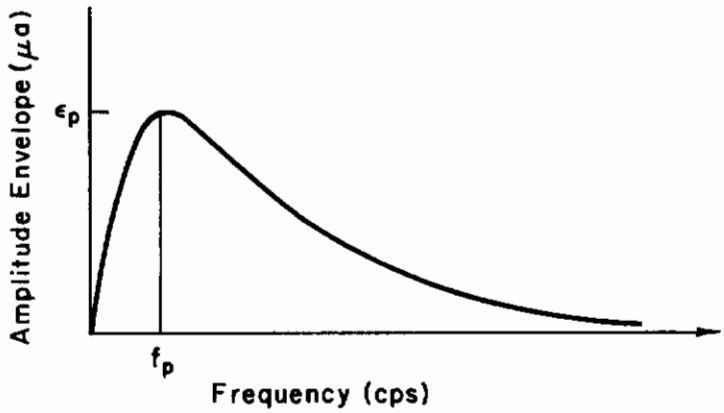

Figure 33. Idealized Deviation Amplitude Envelope

The peak amplitude occurred at f_p = 1 cps, and the amplitude at 10 cps was about 4 percent of peak. Peak deviation, ϵ_p, can be estimated from Figs. 28 through 31. The equation of the envelope as a function of

frequency, f, was assumed to be

$$\epsilon = \left[\frac{Kf}{f^2 + f_p^2}\right]^2$$

The complete disturbance at the receiver output (filtered, with T = 0.5) had the form of Fig. 34 (from Fig. 25 of Ref. 11). Since frequency and time are linearly related by Fig. 32, the time history has the same waveform. Only the center portion of Fig. 34 is of low enough frequency to significantly disturb the aircraft. Typical examples of

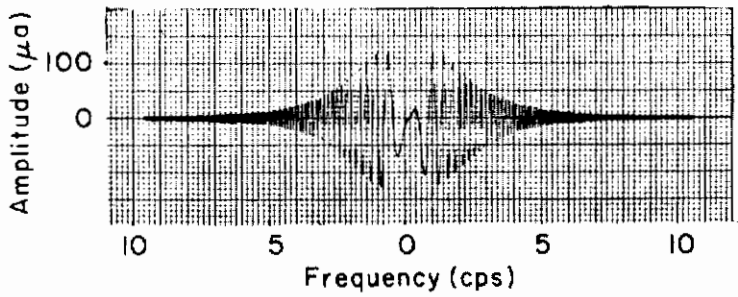

Figure 34. Idealized Deviation Signal

these "low frequency" deterministic waveforms are given in Fig. 35 (taken from Fig. 26 of Ref. 11). As noted in Ref. 11, (a) and (b) have a nonzero average value and may represent a more serious type of deviation than (c). The waveforms of Fig. 35, properly scaled, represent the overflight disturbance as an FCS command input to be modeled analytically or simulated, as the case may be.

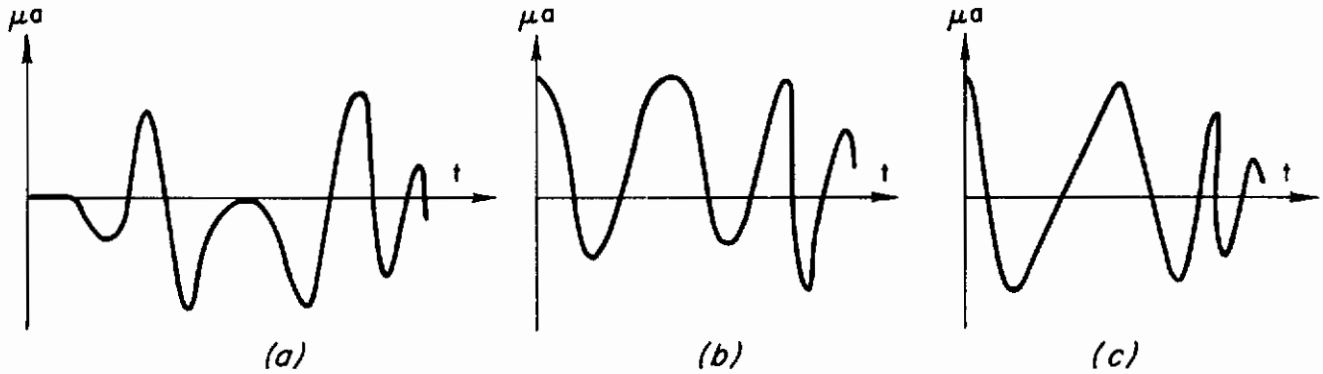

Figure 35. Typical Low Frequency Waveforms

APPENDIX C

NOTS COURSE 10 PROFILE

TABLE IV

NOTS COURSE 10 PROFILE

(All dimensions in feet)

RANGE	ALT.	RANGE	ALT.	RANGE	ALT.	RANGE	ALT.	RANGE	ALT.
54173.	415.	68573.	800.	85872.	4000.	100989.	6700.	114208.	4200.
54897.	420.	70520.	900.	86418.	3900.	101640.	6800.	114407.	4100.
56033.	425.	71177.	1000.	86585.	4000.	101937.	6775.	115516.	4000.
56433.	430.	71642.	1100.	86802.	4100.	102235.	6800.	115752.	3900.
56749.	435.	72083.	1200.	87088.	4200.	102589.	6895.	115975.	3800.
57128.	440.	72405.	1400.	87404.	4300.	103339.	6800.	116143.	3700.
57657.	445.	72560.	1425.	87993.	4400.	104207.	6700.	116397.	3600.
58247.	450.	72628.	1400.	88408.	4500.	104982.	6600.	116763.	3500.
58759.	455.	72808.	1500.	88593.	4525.	105701.	6500.	117042.	3600.
59433.	460.	72932.	1600.	88774.	4500.	106135.	6400.	117290.	3700.
59695.	475.	73050.	1700.	89000.	4450.	106420.	6300.	117519.	3800.
60083.	470.	73341.	1800.	89307.	4500.	106588.	6200.	117606.	3900.
60397.	475.	73695.	1850.	89392.	4525.	106761.	6100.	117823.	4000.
60747.	480.	74030.	1800.	89462.	4500.	106966.	6000.	118070.	4050.
61290.	500.	74495.	1900.	89748.	4600.	107109.	5900.	118319.	4000.
61702.	520.	74842.	2000.	89977.	4700.	107220.	5800.	119150.	3900.
62073.	540.	74972.	2100.	90163.	4800.	107375.	5700.	119665.	3800.
62485.	560.	75332.	2200.	90293.	4900.	107530.	5600.	120092.	3700.
62735.	580.	75815.	2300.	90659.	5000.	107667.	5500.	120371.	3600.
63064.	600.	76299.	2400.	90919.	5100.	107760.	5400.	120756.	3500.
63716.	640.	76975.	2300.	91273.	5200.	108150.	5380.	121233.	3400.
63990.	650.	77793.	2400.	91701.	5300.	108411.	5400.	121760.	3300.
64245.	680.	78047.	2500.	91936.	5400.	108622.	5425.	122060.	3350.
64348.	690.	78314.	2600.	92432.	5500.	108832.	5400.	122262.	3300.
64452.	680.	78525.	2700.	93082.	5550.	109074.	5300.	122777.	3200.
64645.	700.	78674.	2800.	93716.	5500.	109266.	5200.	123478.	3100.
64895.	740.	79263.	2900.	94199.	5400.	109477.	5100.	124532.	3000.
65099.	760.	80261.	2800.	94404.	5500.	109700.	5000.	124720.	2950.
65207.	770.	80410.	2775.	95054.	5525.	109849.	4900.	124904.	3000.
65328.	760.	80577.	2800.	95520.	5500.	110048.	4800.	125542.	3100.
65528.	780.	81160.	2900.	95743.	5525.	110327.	4700.	125700.	3125.
65752.	800.	81358.	3000.	95967.	5500.	110660.	4650.	125834.	3100.
65897.	820.	81842.	3100.	96233.	5600.	111089.	4700.	126082.	3000.
65975.	830.	82208.	3000.	97039.	5700.	111852.	4800.	126232.	3050.
66045.	820.	82344.	3100.	97467.	5800.	112000.	4825.	126386.	3000.
66075.	815.	82499.	3200.	97802.	5900.	112243.	4800.	126547.	2900.
66102.	820.	82716.	3300.	98317.	6000.	112639.	4700.	126851.	2800.
66185.	830.	83188.	3400.	98658.	6100.	112800.	4725.	127000.	2850.
66271.	820.	83764.	3500.	98986.	6200.	112968.	4700.	127248.	2800.
66664.	800.	84211.	3600.	99377.	6300.	113272.	4600.	127458.	2700.
66966.	780.	84583.	3700.	99594.	6400.	113470.	4500.	127900.	2650.
67604.	770.	84868.	3800.	100059.	6500.	113749.	4400.	128345.	2700.
68242.	780.	85159.	3900.	100425.	6600.	114041.	4300.	128674.	2800.

Table IV (Continued)

RANGE	ALT.	RANGE	ALT.	RANGE	ALT.	RANGE	ALT.	RANGE	ALT.
129108.	2900.	145192.	3300.	158994.	5000.	171345.	3900.	180701.	4000.
129399.	3000.	145582.	3330.	159204.	5100.	171550.	3860.	181166.	4100.
129703.	3100.	146060.	3300.	159372.	5200.	171754.	3900.	181371.	4200.
130007.	3200.	147510.	3400.	159558.	5300.	171915.	4000.	181538.	4300.
130232.	3225.	147810.	3375.	160407.	5400.	172219.	4100.	181625.	4315.
130453.	3200.	148100.	3400.	160582.	5450.	172535.	4000.	181712.	4300.
130720.	3100.	148651.	3500.	160736.	5400.	172670.	3985.	181892.	4200.
131253.	3000.	149290.	3600.	160862.	5380.	172802.	4000.	182065.	4100.
132003.	3100.	149563.	3700.	160996.	5400.	173093.	4100.	182332.	4000.
132487.	3200.	149991.	3800.	161722.	5300.	173279.	4200.	182605.	3900.
132977.	3300.	150561.	3900.	161976.	5200.	173412.	4250.	182707.	3885.
133169.	3400.	150728.	4000.	162602.	5100.	173527.	4200.	182816.	3900.
133336.	3500.	150914.	4020.	163297.	5000.	174209.	4100.	183032.	3970.
133510.	3600.	151101.	4000.	163501.	4900.	174316.	4050.	183256.	3900.
133585.	3650.	151408.	4030.	163644.	4800.	174426.	4100.	183496.	3885.
133659.	3600.	151714.	4000.	163787.	4700.	174588.	4000.	183739.	3900.
133894.	3500.	152024.	3900.	164004.	4600.	174767.	4100.	184173.	3800.
134322.	3600.	152163.	3980.	164089.	4580.	175102.	4200.	184203.	3815.
134676.	3700.	152310.	3900.	164165.	4600.	175263.	4300.	184335.	3800.
134998.	3800.	152508.	4000.	164351.	4700.	175679.	4375.	184688.	3700.
136040.	3700.	152647.	4030.	164518.	4800.	175877.	4300.	184800.	3725.
136461.	3600.	152793.	4000.	164884.	4900.	175929.	4280.	184936.	3700.
136852.	3500.	152954.	4020.	165089.	4880.	175989.	4300.	185237.	3615.
137491.	3600.	153134.	4000.	165293.	4900.	176100.	4280.	185538.	3700.
138222.	3500.	153357.	3900.	165400.	4875.	176206.	4300.	185678.	3715.
138371.	3400.	153562.	3870.	165504.	4900.	176466.	4400.	185817.	3700.
138483.	3300.	153773.	3900.	165702.	5000.	176634.	4500.	185965.	3675.
138633.	3275.	154238.	3800.	166143.	5100.	176876.	4600.	186102.	3700.
138811.	3300.	154443.	3900.	166415.	5200.	177198.	4700.	186175.	3715.
138962.	3275.	154647.	4000.	166665.	5250.	177378.	4800.	186257.	3700.
139115.	3300.	155050.	4100.	166930.	5200.	177539.	4900.	186498.	3660.
139264.	3400.	155246.	4125.	167507.	5100.	177843.	5000.	186709.	3700.
139382.	3500.	155435.	4100.	167897.	5000.	178000.	5050.	186859.	3685.
139562.	3550.	155708.	4120.	168437.	4900.	178209.	5000.	187013.	3700.
139741.	3500.	155893.	4100.	168716.	4800.	178779.	4900.	187478.	3800.
139903.	3400.	156327.	4200.	168902.	4700.	179021.	4800.	187714.	3900.
140355.	3300.	156941.	4300.	169522.	4600.	179219.	4700.	187950.	3885.
140625.	3320.	157499.	4400.	169795.	4500.	179412.	4600.	188197.	3900.
140895.	3300.	157878.	4500.	170068.	4400.	179672.	4500.	188495.	4000.
141415.	3200.	158119.	4600.	170272.	4300.	179877.	4400.	188650.	3985.
142693.	3200.	158398.	4700.	170458.	4200.	180038.	4300.	188985.	4000.
144497.	3300.	158659.	4800.	170712.	4100.	180249.	4200.	189320.	4100.
144848.	3320.	158845.	4900.	170991.	4000.	180397.	4100.	189655.	4200.

Table IV (Continued)

RANGE	ALT.	RANGE	ALT.	RANGE	ALT.	RANGE	ALT.	RANGE	ALT.
189895.	4215.	201473.	3800.	215050.	4175.	223960.	4815.	233721.	3900.
190095.	4200.	201770.	3725.	215188.	4200.	224123.	4900.	233850.	3915.
190273.	4125.	202062.	3800.	215957.	4300.	224315.	5000.	233975.	3900.
190448.	4200.	202669.	3900.	216223.	4400.	224480.	5015.	234085.	3910.
190702.	4300.	203339.	4000.	216465.	4500.	224650.	5000.	234192.	3900.
190888.	4400.	204083.	3900.	216738.	4600.	224836.	4900.	234282.	3910.
191037.	4500.	204604.	3800.	216918.	4700.	224922.	4800.	234372.	3900.
191186.	4600.	204734.	3815.	217040.	4715.	225028.	4700.	234775.	3800.
191322.	4700.	204864.	3800.	217166.	4700.	225164.	4600.	234850.	3815.
191620.	4800.	205120.	3760.	217415.	4650.	225332.	4500.	234917.	3800.
191760.	4815.	205348.	3800.	217687.	4700.	225629.	4400.	234997.	3785.
191881.	4800.	205720.	3900.	217941.	4800.	225700.	4425.	235060.	3800.
192079.	4700.	205931.	4000.	218056.	4815.	225784.	4400.	235470.	3835.
192414.	4600.	206340.	4100.	218170.	4800.	225930.	4350.	235879.	3800.
192730.	4700.	207047.	4200.	218424.	4700.	226094.	4400.	236000.	3815.
192879.	4800.	207406.	4300.	218550.	4715.	226289.	4415.	236114.	3800.
193307.	4900.	207679.	4400.	218660.	4700.	226485.	4400.	236263.	3785.
193561.	5000.	207977.	4500.	218750.	4685.	227074.	4500.	236412.	3800.
193871.	5100.	208206.	4600.	218846.	4700.	227291.	4400.	236778.	3900.
193973.	5125.	208280.	4610.	219015.	4675.	227450.	4315.	237187.	3800.
194075.	5100.	208361.	4600.	219175.	4700.	227601.	4400.	237509.	3700.
194187.	5000.	208578.	4500.	219325.	4715.	227818.	4500.	237844.	3600.
194572.	4900.	209025.	4400.	219634.	4700.	227979.	4600.	238917.	3500.
194770.	4800.	209328.	4500.	219844.	4800.	228237.	4615.	239300.	3450.
195099.	4700.	209496.	4600.	220012.	4900.	228506.	4600.	239673.	3500.
195180.	4680.	209707.	4700.	220300.	4950.	228742.	4500.	239900.	3485.
195260.	4700.	210339.	4800.	220905.	4900.	229102.	4400.	240138.	3500.
195774.	4600.	210488.	4830.	221155.	4885.	229455.	4300.	240653.	3600.
196041.	4500.	210637.	4800.	221301.	4900.	229914.	4200.	240765.	3625.
196357.	4400.	210860.	4700.	221537.	4800.	230397.	4100.	240882.	3600.
196525.	4300.	211046.	4600.	221586.	4785.	231098.	4000.	241558.	3700.
196754.	4200.	211319.	4500.	221636.	4800.	231204.	3985.	241700.	3685.
197231.	4100.	211765.	4400.	222002.	4900.	231309.	4000.	241850.	3700.
197839.	4000.	212218.	4300.	222060.	4925.	231415.	4015.	242414.	3800.
198060.	3925.	212943.	4200.	222120.	4900.	231520.	4000.	242953.	3700.
198360.	4000.	213278.	4100.	222319.	4915.	232940.	3900.	243005.	3685.
198980.	4100.	213386.	4075.	222517.	4900.	233125.	3875.	243065.	3700.
199240.	4175.	213495.	4100.	222650.	4875.	233312.	3900.	243300.	3800.
199507.	4100.	213774.	4200.	222777.	4900.	233444.	3885.	243460.	3850.
199743.	4000.	214084.	4300.	222976.	5000.	233473.	3900.	243629.	3800.
200139.	3900.	214450.	4400.	223125.	5025.	233560.	3915.	243842.	3785.
200509.	3925.	214686.	4300.	223217.	5000.	233640.	3900.	244082.	3800.
200877.	3900.	214878.	4200.	223775.	4900.	233680.	3885.	244220.	3815.

Table IV (Concluded)

RANGE	ALT.	RANGE	ALT.	RANGE	ALT.	RANGE	ALT.	RANGE	ALT.
244330.	3800.	254870.	4900.	265950.	3400.	274915.	3550.	284304.	2800.
244751.	3700.	255056.	5000.	266161.	3500.	275022.	3600.	284533.	2900.
244880.	3650.	255261.	5100.	266540.	3600.	275177.	3700.	284750.	2985.
245018.	3700.	255460.	5192.	266790.	3525.	275499.	3800.	284973.	2900.
245170.	3800.	256352.	5100.	267054.	3600.	275859.	3700.	285080.	2915.
245359.	3700.	256693.	5000.	267228.	3700.	276200.	3750.	285197.	2900.
245750.	3600.	256935.	4900.	267370.	3800.	276553.	3700.	285339.	3000.
246150.	3550.	257016.	4800.	267525.	3900.	276925.	3600.	285513.	3100.
246562.	3600.	257165.	4700.	267718.	4000.	277248.	3500.	285854.	3200.
246725.	3625.	257295.	4600.	267826.	4015.	277514.	3400.	285960.	3215.
246903.	3600.	257450.	4500.	267935.	4000.	277750.	3450.	286077.	3200.
247380.	3500.	257741.	4400.	268251.	3900.	278078.	3400.	286393.	3100.
247628.	3400.	258002.	4300.	268511.	3800.	278185.	3375.	286691.	3000.
248340.	3350.	258237.	4200.	268734.	3700.	278289.	3400.	287000.	3100.
249054.	3400.	258498.	4100.	268902.	3600.	278529.	3450.	288042.	3000.
249364.	3500.	258820.	4000.	269045.	3575.	278742.	3400.	288278.	2900.
249538.	3600.	258938.	3900.	269181.	3600.	279157.	3300.	288756.	2800.
249736.	3700.	259075.	3925.	269348.	3700.	279275.	3275.	289100.	2820.
249885.	3725.	259248.	3900.	269675.	3750.	279368.	3300.	289431.	2800.
250034.	3700.	259390.	3915.	269999.	3700.	279448.	3315.	289958.	2700.
250430.	3785.	259552.	3900.	270179.	3800.	279529.	3300.	290045.	2600.
250828.	3700.	259750.	3800.	270309.	3900.	279600.	3285.	290345.	2515.
251088.	3600.	259998.	3700.	270366.	3915.	279666.	3300.	290678.	2600.
251240.	3550.	260172.	3600.	270433.	3900.	279740.	3315.	290900.	2615.
251404.	3600.	260352.	3500.	270766.	3815.	279802.	3300.	291112.	2600.
251609.	3700.	260507.	3400.	271128.	3900.	279859.	3290.	291620.	2500.
251775.	3750.	260675.	3325.	271275.	3885.	279914.	3300.	291719.	2400.
251956.	3700.	260841.	3400.	271407.	3900.	280131.	3200.	292240.	2300.
252135.	3650.	261424.	3500.	271649.	4000.	280200.	3185.	292320.	2285.
252316.	3700.	261796.	3400.	272200.	4100.	280286.	3200.	292401.	2300.
252496.	3800.	261988.	3300.	272386.	4200.	280316.	3210.	292660.	2350.
252824.	3900.	262250.	3215.	272566.	4300.	280447.	3200.	293040.	2300.
253016.	4000.	262540.	3300.	272670.	4315.	281040.	3230.	293877.	2200.
253221.	4100.	262714.	3400.	272771.	4300.	281563.	3200.	000000.	000000
253382.	4200.	263247.	3500.	272932.	4200.	282010.	3100.	000000.	000000
253519.	4300.	263669.	3600.	273093.	4100.	282080.	3085.	000000.	000000
253649.	4400.	264214.	3700.	273546.	4000.	282140.	3100.	000000.	000000
253804.	4500.	264475.	3750.	273775.	3950.	282390.	3120.	000000.	000000
253950.	4515.	264822.	3700.	273856.	4000.	282543.	3100.	000000.	000000
254114.	4500.	265008.	3600.	274395.	3900.	282785.	3000.	000000.	000000
254300.	4600.	265200.	3500.	274588.	3800.	282895.	3015.	000000.	000000
254492.	4700.	265547.	3400.	274687.	3700.	283002.	3000.	000000.	000000
254684.	4800.	265748.	3350.	274805.	3600.	283863.	2900.	000000.	000000

APPENDIX D

ANALYSIS OF TERRAIN SPECTRAL DENSITY DATA

The principal component in the command input during terrain following derives from the terrain itself. The most useful terrain descriptors are those resulting from its characterization as a finite sample of a stationary random process. The terrain following sensor–processor package normally produces a flight path angle command, γ_c, to the flight control system. Spectral densities of γ_c due to the random terrain input can be obtained as a function of aircraft velocity. Representative examples of these are derived for use in performance assessment during flight control system preliminary design.

The material in this appendix is based only on unclassified results of Cornell Aeronautical Laboratory studies. This permits wider access and ease of use, but does not limit the accuracy of the material presented herein or its general utility in FCS preliminary design. The classified literature generally relates to techniques and the performance of specific systems, not the basic terrain data. A definitive summary of classified material related to the description of the FCS command input is provided by Refs. 47–51.

A technique has been developed (Ref. 49) to compute the ideal flight path angle to be flown over a given terrain to optimize the clearance. The resultant flight path is called the "ideal profile." It is a function of the positive and negative load factor limits and the aircraft velocity. Since it defines the ideal or optimum command input, the characteristics of the ideal profile are highly pertinent.

If the actual terrain approximates a stationary random process, so will the ideal profile, because it represents the filtered terrain. Controversy exists as to the degree of Gaussianness present in actual terrain because of its "cuspy" nature (i.e., the valleys are rounded and the hills are peaked). Computation of the ideal profile eliminates the cusps, and the resultant flight path angle command is more nearly Gaussian.

A representative segment of well-known terrain obtained by CAL in Southern Pennsylvania (6201 data) is presented in Fig. 36 (unclassified excerpt from Ref. 49). The ideal profiles are given at three Mach numbers, for zero offset, and with acceleration limits of +1g and −0.5g. The terrain is moderately rough. Reduction of the cuspiness in the ideal profile is evident.

The power distribution of γ_c for several ideal profile trajectories above the 6201 terrain are presented in Fig. 37 (unclassified excerpt from Ref. 49). Similar results are given in Fig. 38 (Ref. 52) for Rocky Mountain terrain (9998 data) ideal profiles. The acceleration limits for both the 6201 and the 9998 profiles were +1g and −0.5g. The 9998 data have more power at both high and low frequencies. The mid-frequency power is about the same. At very low speeds the distribution of the ideal profile would approach that of the actual terrain.

Power spectral densities of the actual terrain profiles are presented in Ref. 48 for both the 6201 and the 9998 data. These data are quite useful in assessing the performance of a given terrain sensor–processor package. It provides a basis, also, for deriving the command input, γ_c, under other normal acceleration conditions or at an arbitrary aircraft velocity.

The power distributions of the ideal profiles in Figs. 37 and 38 have been converted to power spectral density form. This was accomplished by dividing by the frequency in accordance with Ref. 52. The γ_c command input spectral densities are presented in Figs. 39 and 40 for the 6201 and 9998 ideal profiles, respectively. The amplitudes are given in power db ($10 \log_{10}$), and an equivalent white noise shaping filter (amplitude ratio $20 \log_{10}$) can be "fit" directly. All the spectra can be characterized by a well-damped second-order shaping filter having the form of Eq 28.

$$G(s) = \frac{K}{s^2 + 2\zeta\omega s + \omega^2} \tag{28}$$

Parameters of the fitted shaping filters are given in Table V.

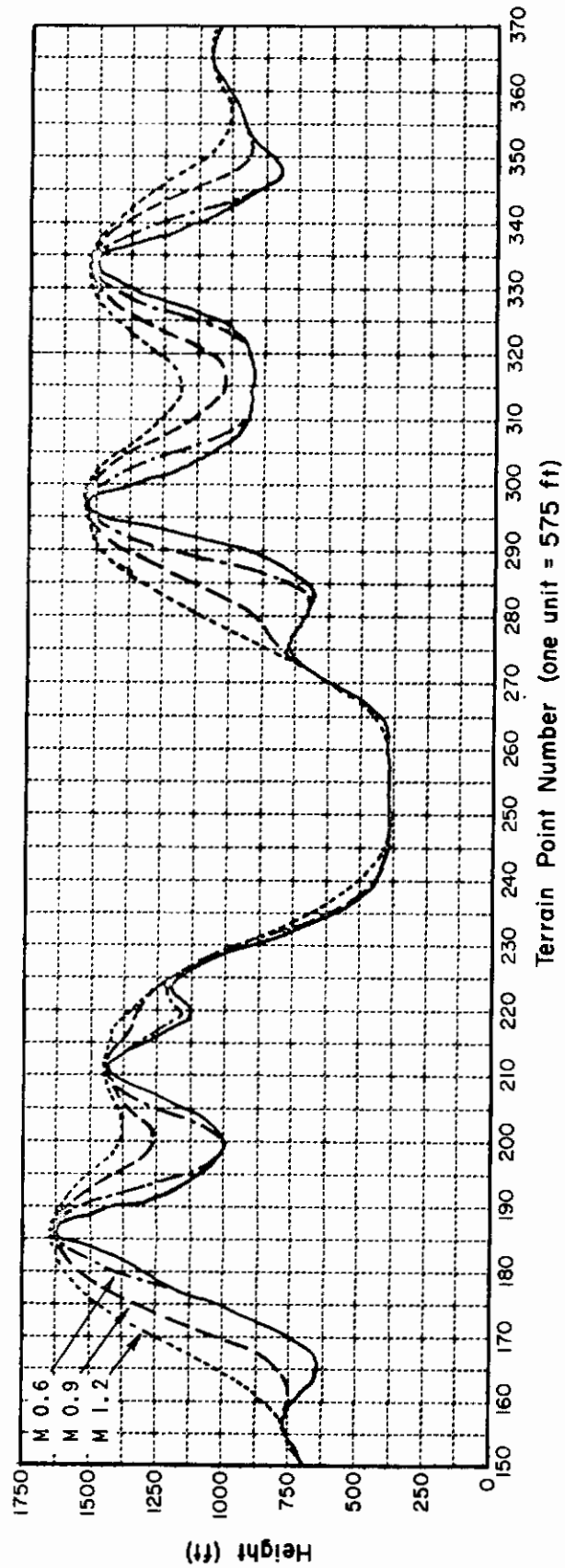

Figure 36. Ideal Profile Trajectories for 6201 Terrain (Ref. 49)

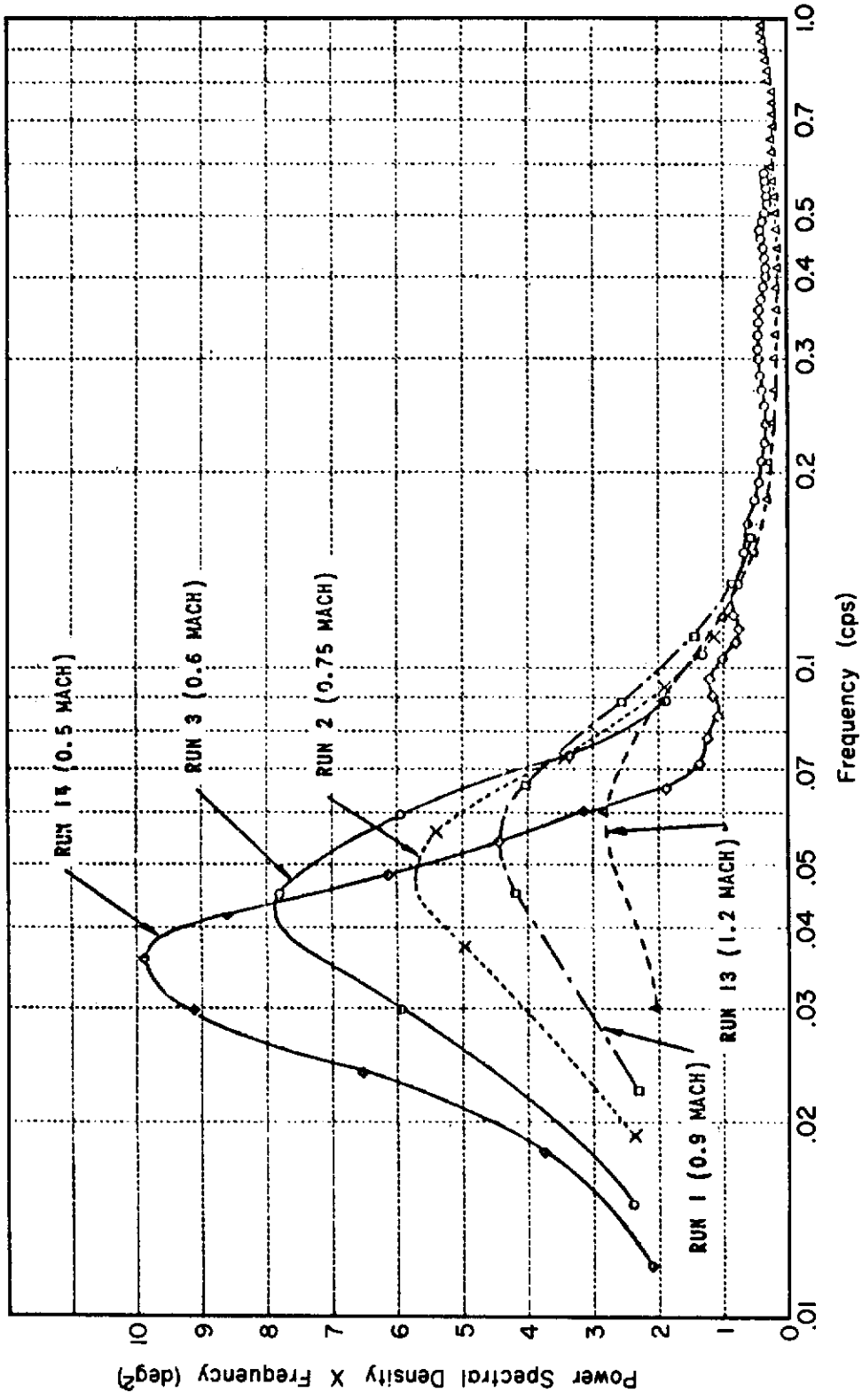

Figure 37. Power Distribution of γ_c for Ideal Profiles (6201 Terrain) (Ref. 49)

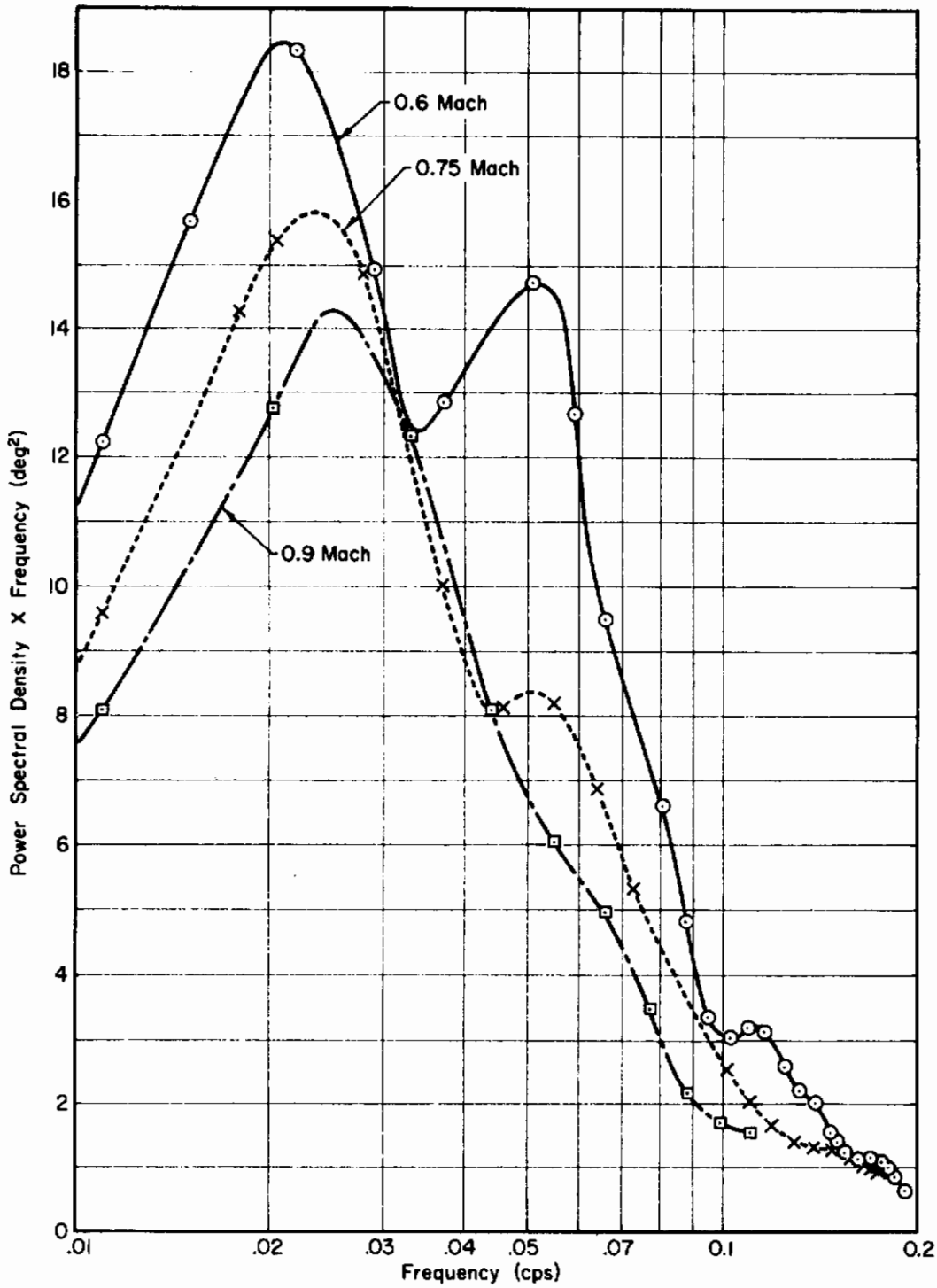

Figure 38. Power Distribution of γ_c for Ideal Profiles (9998 Terrain) (Ref. 52)

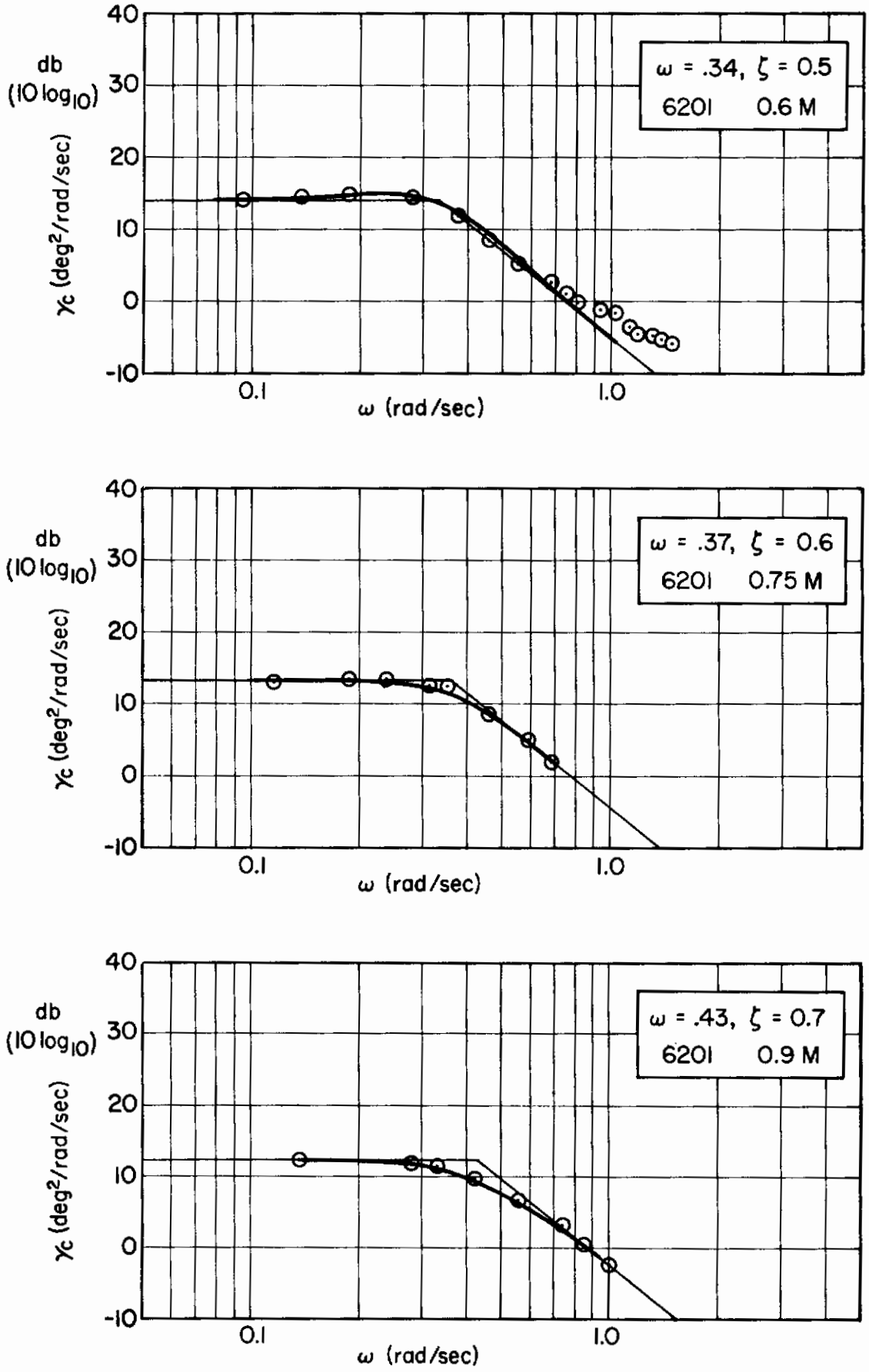

Figure 39. Power Spectral Densities of γ_c for Ideal Profiles (6201 Terrain)

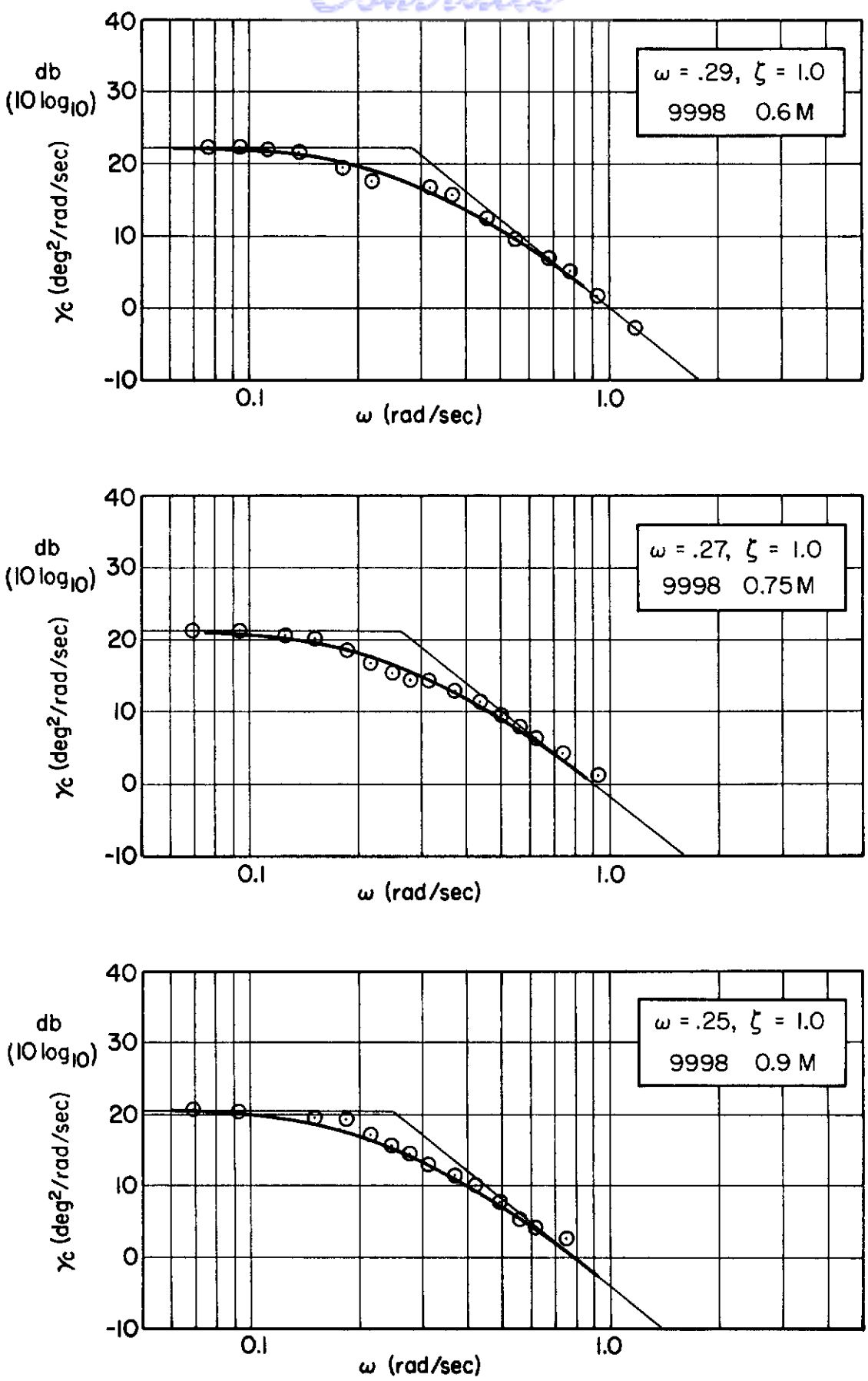

Figure 40 . Power Spectral Densities of γ_c for Ideal Profiles (9998 Terrain)

TABLE V

FILTER PARAMETERS FOR IDEAL PROFILE SPECTRAL DENSITIES

Terrain	0.6 Mach			0.75 Mach			0.9 Mach		
	K	ζ	ω	K	ζ	ω	K	ζ	ω
6201	0.588	0.5	0.34	0.615	0.6	0.37	0.777	0.7	0.43
9998	1.05	1.0	0.29	0.868	1.0	0.27	0.669	1.0	0.25

Unclassified
Security Classification

DOCUMENT CONTROL DATA - R&D

(Security classification of title, body of abstract and indexing annotation must be entered when the overall report is classified)

1. ORIGINATING ACTIVITY *(Corporate author)*
Systems Technology, Inc.
13766 South Hawthorne Boulevard
Hawthorne, California 90250

2a. REPORT SECURITY CLASSIFICATION
Unclassified

2b. GROUP

3. REPORT TITLE
COMPILATION AND ANALYSIS OF FLIGHT CONTROL SYSTEM COMMAND INPUTS

4. DESCRIPTIVE NOTES *(Type of report and inclusive dates)*
Final Report — 1 May 64 — 30 April 65

5. AUTHOR(S) *(Last name, first name, initial)*
Weir, David H.

6. REPORT DATE	7a. TOTAL NO. OF PAGES	7b. NO. OF REFS
January 1966	82	52

8a. CONTRACT OR GRANT NO.	9a. ORIGINATOR'S REPORT NUMBER(S)
AF 33(615)-1818	AFFDL-TR-65-119
b. PROJECT NO. 8219	
c. Task Nr. 821904	9b. OTHER REPORT NO(S) *(Any other numbers that may be assigned this report)*
d.	STI TR-142-1

10. AVAILABILITY/LIMITATION NOTICES
This report will be available to the Clearing-house for Federal Scientific and Technical Information

11. SUPPLEMENTARY NOTES	12. SPONSORING MILITARY ACTIVITY
	AFFDL (FDCC) Wright-Patterson AFB, Ohio

13. ABSTRACT

Flight control command input data are presented for automatic approach and landing, automatic terrain following, and manual control. The data are reduced to analytical forms useful in preliminary design where possible, e.g., servoanalysis methods and approximation techniques appropriate to the use of the data are discussed. Preferred data forms and areas of continuing data need are summarized.

DD FORM 1 JAN 64 1473

Unclassified
Security Classification

14. KEY WORDS	LINK A		LINK B		LINK C	
	ROLE	WT	ROLE	WT	ROLE	WT
Flight control Command input data						

INSTRUCTIONS

1. ORIGINATING ACTIVITY: Enter the name and address of the contractor, subcontractor, grantee, Department of Defense activity or other organization *(corporate author)* issuing the report.

2a. REPORT SECURITY CLASSIFICATION: Enter the overall security classification of the report. Indicate whether "Restricted Data" is included. Marking is to be in accordance with appropriate security regulations.

2b. GROUP: Automatic downgrading is specified in DoD Directive 5200.10 and Armed Forces Industrial Manual. Enter the group number. Also, when applicable, show that optional markings have been used for Group 3 and Group 4 as authorized.

3. REPORT TITLE: Enter the complete report title in all capital letters. Titles in all cases should be unclassified. If a meaningful title cannot be selected without classification, show title classification in all capitals in parenthesis immediately following the title.

4. DESCRIPTIVE NOTES: If appropriate, enter the type of report, e.g., interim, progress, summary, annual, or final. Give the inclusive dates when a specific reporting period is covered.

5. AUTHOR(S): Enter the name(s) of author(s) as shown on or in the report. Enter last name, first name, middle initial. If military, show rank and branch of service. The name of the principal author is an absolute minimum requirement.

6. REPORT DATE: Enter the date of the report as day, month, year, or month, year. If more than one date appears on the report, use date of publication.

7a. TOTAL NUMBER OF PAGES: The total page count should follow normal pagination procedures, i.e., enter the number of pages containing information.

7b. NUMBER OF REFERENCES: Enter the total number of references cited in the report.

8a. CONTRACT OR GRANT NUMBER: If appropriate, enter the applicable number of the contract or grant under which the report was written.

8b, 8c, & 8d. PROJECT NUMBER: Enter the appropriate military department identification, such as project number, subproject number, system numbers, task number, etc.

9a. ORIGINATOR'S REPORT NUMBER(S): Enter the official report number by which the document will be identified and controlled by the originating activity. This number must be unique to this report.

9b. OTHER REPORT NUMBER(S): If the report has been assigned any other report numbers *(either by the originator or by the sponsor)*, also enter this number(s).

10. AVAILABILITY/LIMITATION NOTICES: Enter any limitations on further dissemination of the report, other than those imposed by security classification, using standard statements such as:

(1) "Qualified requesters may obtain copies of this report from DDC."

(2) "Foreign announcement and dissemination of this report by DDC is not authorized."

(3) "U. S. Government agencies may obtain copies of this report directly from DDC. Other qualified DDC users shall request through _____."

(4) "U. S. military agencies may obtain copies of this report directly from DDC. Other qualified users shall request through _____."

(5) "All distribution of this report is controlled. Qualified DDC users shall request through _____."

If the report has been furnished to the Office of Technical Services, Department of Commerce, for sale to the public, indicate this fact and enter the price, if known.

11. SUPPLEMENTARY NOTES: Use for additional explanatory notes.

12. SPONSORING MILITARY ACTIVITY: Enter the name of the departmental project office or laboratory sponsoring *(paying for)* the research and development. Include address.

13. ABSTRACT: Enter an abstract giving a brief and factual summary of the document indicative of the report, even though it may also appear elsewhere in the body of the technical report. If additional space is required, a continuation sheet shall be attached.

It is highly desirable that the abstract of classified reports be unclassified. Each paragraph of the abstract shall end with an indication of the military security classification of the information in the paragraph, represented as *(TS), (S), (C), or (U)*.

There is no limitation on the length of the abstract. However, the suggested length is from 150 to 225 words.

14. KEY WORDS: Key words are technically meaningful terms or short phrases that characterize a report and may be used as index entries for cataloging the report. Key words must be selected so that no security classification is required. Identifiers, such as equipment model designation, trade name, military project code name, geographic location, may be used as key words but will be followed by an indication of technical context. The assignment of links, rules, and weights is optional.